Clim. Past, 6, 345–365, 2010
www.clim-past.net/6/345/2010/
doi:10.5194/cp-6-345-2010

Climate of the Past

Millennial and sub-millennial scale climatic variations recorded in polar ice cores over the last glacial period

E. Capron[1], A. Landais[1], J. Chappellaz[2], A. Schilt[3], D. Buiron[2], D. Dahl-Jensen[4], S. J. Johnsen[4], J. Jouzel[1], B. Lemieux-Dudon[2], L. Loulergue[2], M. Leuenberger[3], V. Masson-Delmotte[1], H. Meyer[5], H. Oerter[5], and B. Stenni[6]

[1]Institut Pierre-Simon Laplace/Laboratoire des Sciences du Climat et de l'Environnement, CEA-UMR INSU/CNRS 8212-UVSQ, 91191 Gif-sur-Yvette, France
[2]Laboratoire de Glaciologie et Géophysique de l'Environnement, CNRS-UJF, 38400 St Martin d'Hères, France
[3]Climate and Environmental Physics, Physics Institute, and Oeschger Centre for Climate Change Research, University of Bern, Sidlerstr. 5, 3012 Bern, Switzerland
[4]Centre for Ice and Climate, Niels Bohr Institute, Univ. of Copenhagen, Juliane Maries Vej 30, 2100, Copenhagen, Denmark
[5]Alfred Wegener Institute for Polar and Marine Research, Bremerhaven, P.O. Box 120161, 27515, Bremerhaven, Germany
[6]University of Trieste, Department of Geosciences, Via E. Weiss 2, 34127 Trieste, Italy

Received: 13 January 2010 – Published in Clim. Past Discuss.: 11 February 2010
Revised: 7 May 2010 – Accepted: 26 May 2010 – Published: 9 June 2010

Abstract. Since its discovery in Greenland ice cores, the millennial scale climatic variability of the last glacial period has been increasingly documented at all latitudes with studies focusing mainly on Marine Isotopic Stage 3 (MIS 3; 28–60 thousand of years before present, hereafter ka) and characterized by short Dansgaard-Oeschger (DO) events. Recent and new results obtained on the EPICA and NorthGRIP ice cores now precisely describe the rapid variations of Antarctic and Greenland temperature during MIS 5 (73.5–123 ka), a time period corresponding to relatively high sea level. The results display a succession of abrupt events associated with long Greenland InterStadial phases (GIS) enabling us to highlight a sub-millennial scale climatic variability depicted by (i) short-lived and abrupt warming events preceding some GIS (precursor-type events) and (ii) abrupt warming events at the end of some GIS (rebound-type events). The occurrence of these sub-millennial scale events is suggested to be driven by the insolation at high northern latitudes together with the internal forcing of ice sheets. Thanks to a recent NorthGRIP-EPICA Dronning Maud Land (EDML) common timescale over MIS 5, the bipolar sequence of climatic events can be established at millennial to sub-millennial timescale. This shows that for extraordinary long stadial durations the accompanying Antarctic warming amplitude cannot be described by a simple linear relationship between the two as expected from the bipolar seesaw concept. We also show that when ice sheets are extensive, Antarctica does not necessarily warm during the whole GS as the thermal bipolar seesaw model would predict, questioning the Greenland ice core temperature records as a proxy for AMOC changes throughout the glacial period.

Correspondence to: E. Capron
(emilie.capron@lsce.ipsl.fr)

1 Introduction

Continental, marine and polar paleoclimate records preserve abundant evidence that a series of abrupt climate events at millennial scale occurred during the last glacial period (∼18–110 thousand years before present, hereafter ka) with different expressions over the entire globe (Voelker, 2002). These so-called "Dansgaard-Oeschger" (DO) events were first described and numbered in the deep Greenland ice cores from Summit back to 100 ka (72°34′ N, 37°37′ W, GISP2 and GRIP; Dansgaard et al., 1993; Grootes et al., 1993; GRIP-members, 1993). GISP2 and GRIP $\delta^{18}O_{ice}$ records highlight millennial scale variability related to the succession of interstadials (defined as the warm phases of the millennial scale variability; hereafter noted GIS for Greenland InterStadial) and stadials (defined as the cold phase of the millennial scale variability; hereafter noted GS for Greenland Stadial; Dansgaard et al., 1993).

Published by Copernicus Publications on behalf of the European Geosciences Union.

The "iconic" DO event structure is depicted as a GIS, beginning with an abrupt warming of 8 to 16 °C in mean annual surface temperature within a few decades (Severinghaus et al., 1998; Lang et al., 1999; Landais et al., 2004a; Huber et al., 2006; Landais et al., 2006; see also Wolff et al., 2009a for a review). The GIS is then usually characterized by a gradual cooling phase lasting several centuries and its end is marked by a rapid cooling towards a relatively stable cold phase (GS) that persists over several centuries to a thousand of years. This description originates mainly from the DO events occurring over Marine Isotopic Stage 3 (MIS 3, 28–60 ka; See Voelker, 2002 for a review) that benefit from a robust chronology (Fig. 1; e.g. Wang et al., 2001; Shackleton et al., 2003a; Fairbanks et al., 2005; Svensson et al., 2008).

The DO event signature is recorded in both continental and marine archives from high northern latitudes to the tropics (e.g. Bond et al., 1992; Sanchez-Goñi et al., 2000; Sanchez-Goñi et al., 2002; Genty et al., 2003; Wang et al., 2008). This mainly northern hemispheric characteristic is also illustrated by abrupt changes in atmospheric methane (CH_4) concentrations inferred from air trapped in ice associated with Greenland temperature shifts (e.g. Chappellaz et al., 1993; Flückiger et al., 2004; Huber et al., 2006; Loulergue et al., 2008).

A dynamical combination between ocean, cryosphere (continental ice sheets and sea ice cover), vegetation and atmosphere is at play during this millennial scale variability (Hendy and Kennett, 1999; Peterson et al., 2000; Kiefer et al., 2001; Wang et al., 2001; Broecker, 2003; Steffensen et al., 2008) but the triggering processes of such a variability are still under discussion (Wunsch, 2006; Friedrich et al., 2009). Current theories point to external forcing mechanisms such as periodic changes in solar activity (Bond et al., 1992; Braun et al., 2008), periodic calving of ice sheets (van Kreveld et al., 2000) and to internal oscillations of the ice sheet-ocean-atmosphere system through freshwater perturbations (Broecker, 1990; MacAyeal, 1993; Ganopolski and Rahmstorf, 2001; Schulz et al., 2002).

In Antarctic ice cores, millennial scale temperature changes are gradual and out of phase with their abrupt northern counterpart (Fig. 1; Bender et al., 1994; Blunier et al., 1998; Blunier and Brook, 2001; EPICA-community-members, 2006; Capron et al., 2010). Such a "bipolar seesaw" pattern is understood as reflecting changes in the strength of the Atlantic Meridional Oceanic Circulation (AMOC; Broecker, 1998). The physical mechanism for this bipolar seesaw pattern has been explored through a large number of conceptual and numerical models of various complexities (e.g. Stocker et al., 1992; Rind et al., 2001; Velinga and Wood, 2002; Knutti et al., 2004; Kageyama et al., 2009; Liu et al., 2009; Swingedouw et al., 2009). Using the simplest possible model, Stocker and Johnsen (2003) successfully described the Antarctic millennial variability in response to the abrupt temperature changes in the north by involving a southern heat reservoir associated with AMOC variations. Such an important role of the Southern Ocean for the bipolar seesaw mechanism is supported by marine records (Barker et al., 2009).

Our knowledge of millennial scale climatic evolution before MIS 3 is limited by lower resolution, as well as higher stratigraphic and dating uncertainties. Nevertheless, millennial scale variability is observed from the very beginning of the last glacial period (Cortijo et al., 1994; McManus et al., 1999; Eynaud et al., 2000; Oppo et al., 2001; Genty et al., 2003; Heusser and Oppo, 2003; NorthGRIP-community-members, 2004; Sprovieri et al., 2006; Meyer et al., 2008; Wang et al., 2008) and during previous glacial periods (McManus et al., 1999; Jouzel et al., 2007; Siddall et al., 2007; Loulergue et al., 2008).

MIS 5 (∼73.5–130 ka; Shackleton, 1987) includes the last glacial inception and the early glacial which are a time period of great interest since they represent an intermediate stage between full interglacial conditions (defined as MIS 5e, Shackleton et al., 2003b; Fig. 1) and glacial conditions encountered during MIS 2–3. At that time, continental ice sheets are extending, corresponding to sea level variations from 20 to 60 m below present-day sea level (Waelbroeck et al., 2002) compared to 120 m below present-day sea level during MIS 2–3. MIS 5 is also marked by a different orbital configuration with stronger eccentricity and therefore larger seasonal insolation changes compared to MIS 3 (Fig. 1).

The NorthGRIP ice core (Greenland, 75° 10′ N, 42° 32′ W; 2917 m a.s.l.; present accumulation rate of 17.5 cm water equivalent per year (cm w.e. yr^{-1})) expands the Summit records back to the last interglacial period (∼123 ka) and offers high resolution (1 cm yr^{-1}) due to the basal melt limiting thinning processes (NorthGRIP c.m., 2004). The $\delta^{18}O_{ice}$ profile unveiled GIS 23, 24, and 25 in the early time of the glacial period (∼101–113 ka; Fig. 1; NorthGRIP c.m., 2004). The discovery of only six abrupt climatic events during MIS 5 (GIS 20 to 25) reveals a longer pacing than the ∼1.5 thousand year (hereafter kyr) approximate DO event frequency suggested by Grootes and Stuiver (1997) between 12 and 50 ka which has been strongly debated (e.g. Grootes and Stuiver, 1997; Schulz, 2002; Rahmstorf, 2003; Ditlevsen et al., 2005, 2007).

We also use here an ice core drilled within the European Project for Ice Coring in Antarctica (EPICA) in the interior of Dronning Maud Land (hereafter, denoted EDML, 75° S, 0° E, 2892 m a.s.l., present accumulation rate of 6.4 cm w.e. yr^{-1}). It represents a South Atlantic counterpart to the Greenland records (EPICA c.m., 2006) and provides a resolution of ∼30 yrs during MIS 3 and of ∼60 yrs during MIS 5 that makes the EDML core particularly suitable for studying millennial scale climatic variations in Antarctica. During MIS 3, it has been shown that the amplitudes of EDML Antarctic Isotopic Maxima (AIM) are linearly related to the duration of the concurrent GS (EPICA c.m., 2006). Moreover, taking advantage of a new common timescale between EDML and NorthGRIP ice cores based on the global signals

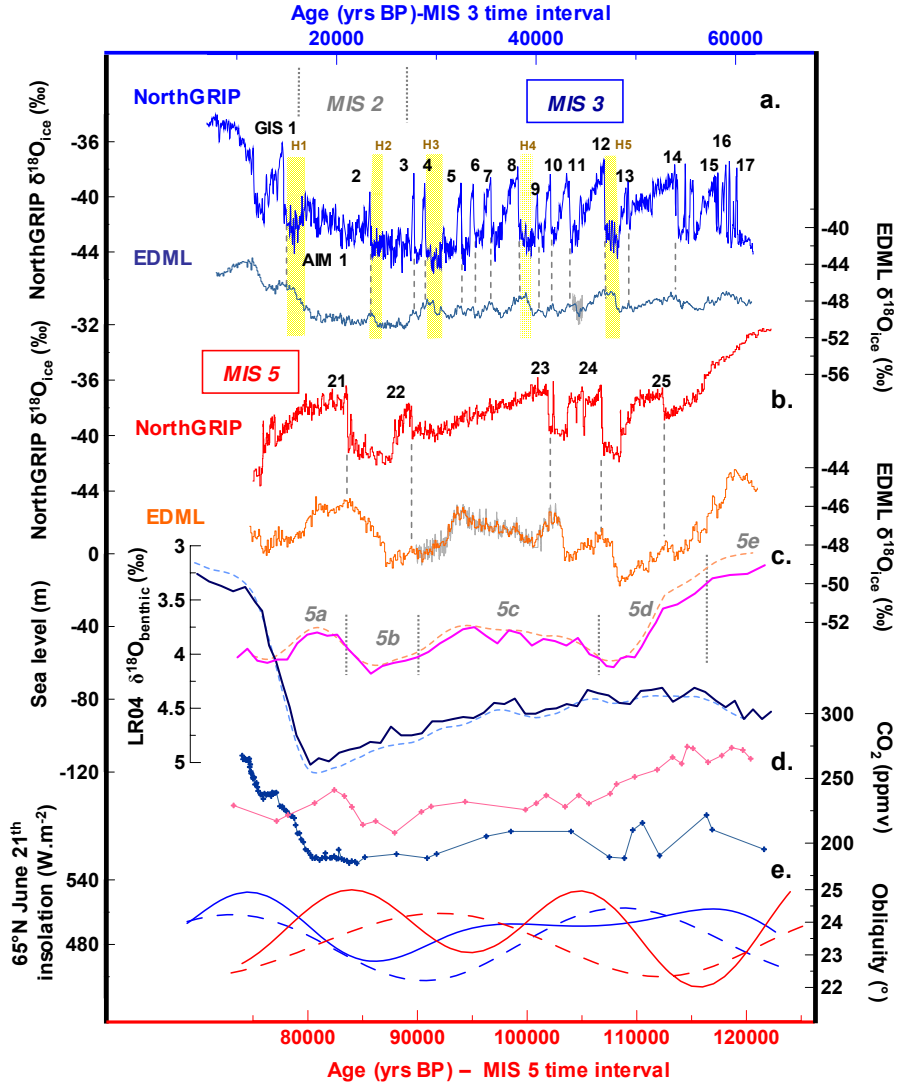

Fig. 1. Comparison of some climatic parameters over MIS 3 and MIS 5. **(a)** MIS 3 NorthGRIP $\delta^{18}O_{ice}$ (light blue curve, NorthGRIP c. m., 2004) and EDML $\delta^{18}O_{ice}$ (dark blue curve, EPICA c.m., 2006; grey curve, this study). **(b)** MIS 5 NorthGRIP $\delta^{18}O_{ice}$ (red curve, NorthGRIP c.m., 2004) and EDML $\delta^{18}O_{ice}$ (orange curve, EPICA c.m., 2006; grey curve, this study). Note that new $\delta^{18}O_{ice}$ measurements on EDML ice core were performed over AIM events 11 and 23 (grey curve) at Alfred Wegener Institute (Germany) with a depth resolution of 0.05 m, using the CO_2 (H_2)/water equilibration technique (Meyer et al., 2000). **(c)** MIS 3 (dotted light blue curve) and MIS 5 (dotted orange curve) sea level variations (Bintanja et al., 2005) reconstructed from the LR04 $\delta^{18}O_{benthic}$ stack (MIS 3, solid dark blue line; MIS 5, solid pink line; Lisiecki and Raymo, 2005). Both the sea level curve and the LR04 $\delta^{18}O_{benthic}$ stack are displayed on EDC3 timescale. The timescale synchronisation is done in Parrenin et al. (2007a). **(d)** MIS 3 (dark blue curve) and MIS 5 (pink curve) CO_2 concentration. Composite CO_2 from EDC and Vostok ice cores (Petit et al., 1999; Monnin et al., 2001; Lüthi et al., 2008). **(e)** MIS 3 and MIS 5 orbital contexts: 65° N summer insolation (full line) and obliquity (dotted line) (Laskar et al., 2004). Heinrich Events (H-events) and Greenland InterStadials (GIS) are indicated on the NorthGRIP record. Dotted grey lines show the one to one coupling observed between AIM and DO events. Marine Isotopic Sub-stages are indicated on the LR04 $\delta^{18}O_{benthic}$ stack. This highlights the close link between the long-term variations of ice sheet volume and the millennial scale variability since the onsets of GIS 24, 22 and 21 correspond to the transition from Marine Isotopic Sub-stages 5d to 5c, 5c to 5b and 5b to 5a, respectively.

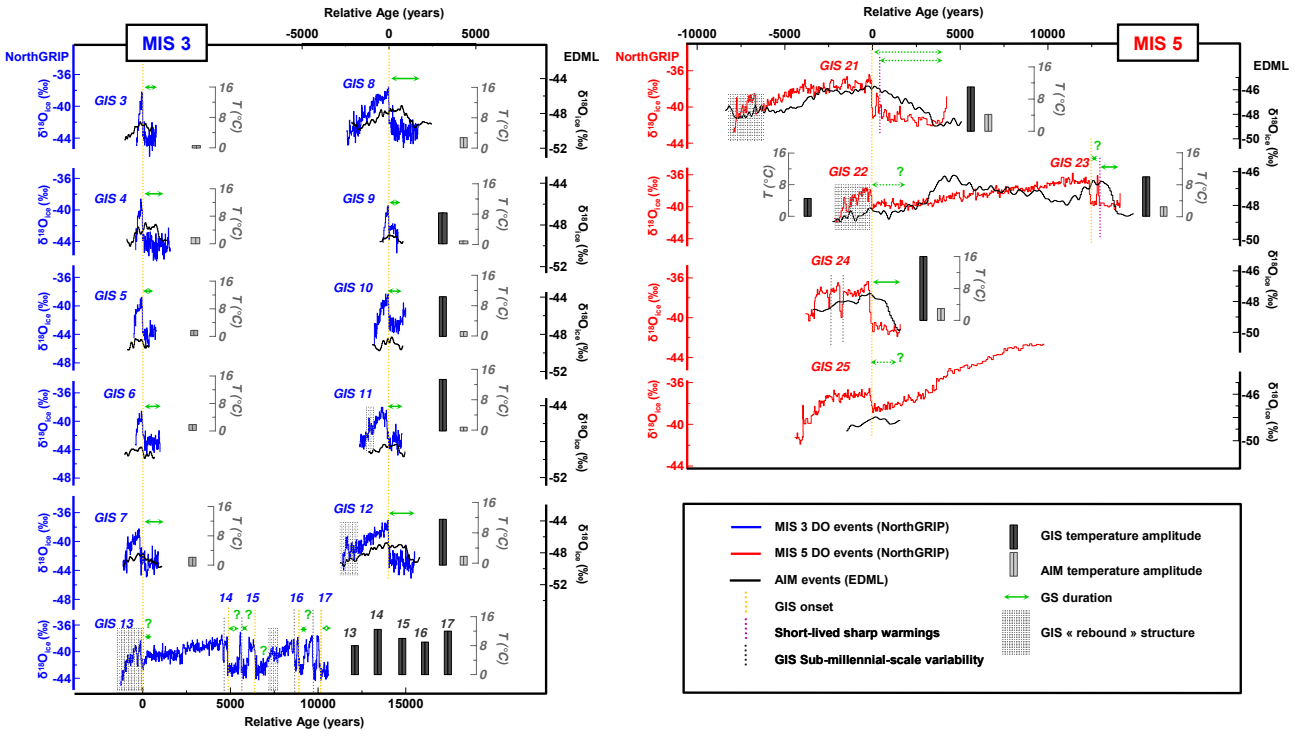

Fig. 2. Synthesis of millennial and sub-millennial scale climatic variability during MIS 3 (blue curve) and MIS 5 (red curve) recorded in NorthGRIP $\delta^{18}O_{ice}$ (NorthGRIP c.m., 20004) on a relative age centred on the onset of Greenland rapid events. AIM events recorded in EDML $\delta^{18}O_{ice}$ are superimposed (EPICA c.m., 2006; grey curve). Vertical dotted bars mark onsets of GIS (yellow) and precursor-type peak events (purple), sub-millennial scale variability over sequence of events 13–17 and GIS 24 (grey). Shaded grey bands indicate rebound-type events. Horizontal green arrows materialise GS duration (in dotted line when the duration is uncertain). Bars represent amplitudes of local temperature increase at the onset of GIS events based on $\delta^{15}N$ measurements (dark bars; Huber et al., 2006; Landais et al. 2006; this study) and AIM warming amplitudes (grey bars; EPICA c.m., 2006; this study).

of atmospheric composition changes, Capron et al. (2010) depict a bipolar seesaw structure during MIS 5 extending down to GIS 25 (Fig. 2). They reveal that during the long GS 22 the corresponding AIM 21 amplitude does not reach the warming expected from the linear relationship observed during MIS 3.

In this paper, we combine the full climatic information available from the NorthGRIP and EPICA ice cores in order to provide a complete description of the abrupt climatic oscillations recorded in the polar regions over MIS 5 in comparison to MIS 3. In Sect. 2, we present the common timescales used for the NorthGRIP and EPICA ice cores over MIS 3 and MIS 5. Section 3 deals with new high resolution measurements of EDML $\delta^{18}O_{ice}$ and of NorthGRIP $\delta^{15}N$ and $\delta^{40}Ar$ which are then used to characterize MIS 5 GS and GIS in terms of structure, temperature amplitude and their relationships with their Antarctic counterparts. In particular, we bring new evidence of sub-millennial scale variability at the onset and the end of the MIS 5 long interstadials. We then discuss the robust features and peculiarities of GIS events of MIS 3 and MIS 5 in relationship with their different climate background (i.e. ice volume, orbital contexts) in Sect. 4. Finally, in Sect. 5, we test the general applicability of the thermal bipolar seesaw concept for the entire glacial period by comparing our results with north-south time-series generated through the conceptual model of Stocker and Johnsen (2003).

2 Timescale synchronisation and past temperature reconstruction of NorthGRIP and EDML ice cores

2.1 Synchronising NorthGRIP and EDML ice cores

An accurate timescale is necessary to characterize the duration and pacing of climatic events and the sequence of events between the Northern and the Southern Hemispheres.

For MIS 3, we use the most recent GICC05 age scale (Greenland Ice Core Chronology 05) extended back to 60 ka (Svensson et al., 2008) for the NorthGRIP ice core. GICC05 is a timescale based on annual layer counting and has been shown to be compatible within the given counting error with absolutely dated reference horizons in the 0–60 ka period (Svensson et al., 2008; Fleitmann et al., 2009) with GICC05 tending to generally underestimate the age. Synchronization (e.g. Bender et al., 1994; Blunier et al., 1998)

Table 1. Uncertainties on MIS 5 DO events duration associated with the new EDML-NorthGRIP common timescale over MIS 5 (Capron et al., 2010). The uncertainty determination is based on the comparison of DO duration inferred from the EDML-NorthGRIP timescale with their duration on other timescales (marine sediment cores: MD95-2042, Shackleton et al. (2004) and NEAP18K, Chapman and Shackelton (2002); Sanbao Cave speleothem record, Wang et al. (2008); lake record from Monticchio, Brauer et al. (2007)).
[a] DO duration on each chronology: (1) EDML-NorthGRIP timescale (2) MD95-2042 timescale (3) NEAP18K timescale, (4) Sambao Cave timescale, (5) Lago di Monticchio timescale.
[b] For each rapid event, we calculate the mean DO duration deduced from DO durations estimated on each chronology (a).
[c] The uncertainty of each event duration is given as a percentage of error calculated as the ratio between the standard deviation of DO durations on each timescale (a) and the mean event duration (b).

	DO duration on each chronology (yrs)[a]					Mean DO[b] duration (yrs)	Event[c] duration uncertainty (%)
	(1) EDML-NGRIP	(2) MD95-2042	(3) NEAP-18 K	(4) Sambao Cave	(5) Monticchio		
DO25	5530	3950	2990	3970	2610	3810	30
DO24	4850	4130	4940	5150	4820	4778	8
DO23	12 570	11 190	11 530	13 900	9460	11 730	14
DO22	5870	6300	4940	6750	5340	5840	12
DO21	9350	6460	9700	7360		8218	19

performed using the isotopic composition of atmospheric oxygen ($\delta^{18}O_{atm}$) and CH_4 records from air entrapped in EDML and NorthGRIP ice (EPICA c.m., 2006; Blunier et al., 2007) allowed us to place the two ice cores on the same timescale. From 25 to 50 ka, the maximum uncertainty between the two records is estimated to reach 500 yrs at the onset of GIS 12.

To study MIS 5, we transfer the NorthGRIP record onto the EDML1 timescale (Parrenin et al., 2007a; Ruth et al., 2007; Severi et al., 2007) between 75 and 123 ka using also a $\delta^{18}O_{atm}$ and CH_4 synchronisation (Capron et al., 2010). The new EDML-NorthGRIP timescale enables us to quantify the exact phasing between the onsets of AIM and GIS with an accuracy of a few centuries except for the onset of GIS 25, where the uncertainty is higher than 1 kyr due to the lack of high-resoluted methane records both on EDML and NorthGRIP that would enable one to determine a precise gas age marker between the two records. Unlike for MIS 3, we are not using an absolute timescale for MIS 5 however focussing on the duration and sequence of events only requires a relative timescale. NorthGRIP basal melting induces a timescale almost linearly proportional to depth by reducing the ice thinning (NorthGRIP c.m., 2004; Dahl-Jensen et al., 2003). For the new EDML-NorthGRIP age-scale, we obtain a smooth evolution of age as a function of depth with less than 10% deviation from the slope deduced from the age/depth relationship of the NorthGRIP glaciological timescale (NorthGRIP c.m., 2004). We thus consider our age markers as being consistent with ice flow conditions at the NorthGRIP site.

We compare this new timescale with independent chronologies from other paleoclimatic archives (Table 1) and this enables us to derive uncertainties associated with the duration of each GIS/GS succession over MIS 5. In the North Atlantic region, marine cores show rapid cooling events (C events) (McManus et al., 1994) that were associated with the GS (i.e. event C 24 is associated with GS 25, McManus et al., 1994; NorthGRIP c.m., 2004; Rousseau et al., 2006). Using such associations, NorthGRIP DO event duration is compared to the one deduced from two marine sediment cores: (i) MD95-2042, providing an age scale with two absolute age markers derived from the Hulu cave between 115 and 81 ka (Shackleton et al., 2003a; Wang et al., 2001) and (ii) NEAP18K, whose age model was constructed by correlation of the benthic $\delta^{18}O$ records with an orbitally tuned $\delta^{18}O$ stratigraphy (Shackleton and Pisias, 1985).

Then, the same exercise is carried out by comparing our age-scale with the chronology from a lacustrine sediment core from Lago grande di Monticchio (Brauer et al., 2007) whose chronology is based on lamination counting. Finally, assuming synchronous climatic shifts at low and high latitudes enables us to compare rapid event succession recorded in ice cores through independent dating from speleothem records (i.e. Wang et al., 2001, 2008). Such a comparison is difficult because few speleothem records display a clear sequence of rapid events over MIS 5 except the record from Sanbao cave on which we can identify the onset of each GIS event (Wang et al., 2008).

Uncertainties on DO event durations (i.e. durations of GIS plus GS) obtained from the comparison of the five records are summarized in Table 1. In the following we limit our study to the sequence of events 24, 23, 22, and 21 since the EDML-NorthGRIP synchronisation lacks of robust chronological constraints around GIS 25 (Capron et al., 2010). The uncertainties associated with the durations of GIS/GS 24, 23, 22 and 21 represent less than 19% of the duration of each DO event. This general agreement makes the

Table 2. North-South rapid events recorded in NorthGRIP and EPICA ice cores.
[a] NorthGRIP $\delta^{18}O_{ice}$ amplitude ($\Delta\delta^{18}O_{ice}$) at the onset of abrupt events (NorthGRIP c.m., 2004).
[b] Accompanying warming amplitude (ΔT) estimated from $\delta^{15}N$ data with associated uncertainty.
[c] Huber et al. (2006) and Landais et al. (2006) provide a quantification of abrupt temperature change through air isotopes measurements of most of the rapid events over the last glacial period and our study provides new results of temperature estimates at the onset of GIS 21 and GIS 22.
[d] Spatial slope deduced at the onset of each rapid event as α=$\Delta\delta^{18}O_{ice}/\Delta T$. Note that a $\pm$2.5 °C uncertainty on temperature change is translated to an error of $\sim$0.2 in the calculation of α.
[e] GS durations are given (1) on the GICC05 age scale for GS 2 to GS 12 (Blunier et al., 2007; Svensson et al., 2008), (2) on ss09sea age scale for GS 18 to GS 20 (NorthGRIP c.m., 2004) and (3)on the EDML-NorthGRIP synchronised timescale for GS 21 to GS 24 (Capron et al., 2010). GS duration is defined by the interval between the midpoint of the stepwise temperature change at the start and end of a stadial. The errors associated with stadial duration are estimated by using different splines through the data that affect the width of the DO transitions and are linked to visual determination of maxima and minima during transitions. No estimate of GS is given where the beginning of the GS is hard to pinpoint due to the particular structure of events and the corresponding events are labeled with #.
[f] AIM warming amplitudes are given for the EDML ice core based on the temperature reconstruction of Stenni et al. (2010). AIM 22 is damped after d-excess corrections and labeled as * (See Stenni et al. (2010) for details). The amplitude is determined following EPICA c.m. (2006) from the Antarctic $\delta^{18}O_{ice}$ maximum to the preceding minimum of each event. Uncertainties on MIS 3 AIM amplitudes are determined in EPICA c.m. (2006). For AIM events during MIS 2, MIS 4 and MIS 5, we consider that an error bar of $\pm$0.4 °C encompasses the uncertainty on the determination of the warming amplitude by using different splines through the data.

DO	NG $\Delta\delta^{18}O_{ice}$ (‰) [a]	NG ΔT (°C) [b]	Reference [c]	NorthGRIP α (‰/°C) [d]	GS Δt (yrs) [e]	AIM	EDML ΔT (°C) [f]	Reference
2	**3.9**				**4100**±100 (1)	**2**	**2**±0.4	This study
3	**5.5**				**800**±150 (1)	**3**	**0.6**±0.2	EPICA c.m., 2006
4	**4.9**				**1600**±250(1)	**4**	**1.8** ±0.2	EPICA c.m., 2006
5	**4.2**				**900** ±150(1)	**5**	**1.1** ±0.2	EPICA c.m., 2006
6	**4.2**				**1000** ±150 (1)	**6**	**1.2** ±0.3	EPICA c.m., 2006
7	**4.2**				**1300** ±250 (1)	**7**	**1.9** ±0.3	EPICA c.m., 2006
8	**4.7**	**11** (+3;−6)	Huber et al., 2006	**0.43**	**1800** ±150 (1)	**8**	**2.7** ±0.3	EPICA c.m., 2006
9	**2.6**	**9** (+3;−6)	Huber et al., 2006	**0.29**	**800**±150 (1)	**9**	**0.8**±0.3	EPICA c.m., 2006
10	**4**	**11.5** (+3;−6)	Huber et al., 2006	**0.35**	**2000**±250(1)	**10**	**1.4** ±0.2	EPICA c.m., 2006
11	**5.4**	**15** (+3;−6)	Huber et al., 2006	**0.33**	**1100** ±150 (1)	**11**	**1.5** ±0.4	This study
12	**5.6**	**12.5** (+3;-6)	Huber et al., 2006	**0.45**	**1600** ±150 (1)	**12**	**2.4** ± 0.4	EPICA c.m., 2006
13	**2.9**	**8** (+3;−6)	Huber et al., 2006	**0.36**	#	**13**		
14	**4.9**	**12**±2.5	Huber et al., 2006	**0.41**	#	**14**		
15	**4**	**10** (+3;−6)	Huber et al., 2006	**0.40**	#	**15**		
16	**3.9**	**9** (+3;−6)	Huber et al., 2006	**0.43**	#	**16**		
17	**4**	**12** (+3;−6)	Huber et al., 2006	**0.33**	#	**17**		
18	**4.5**	**11** ±2.5	Landais et al., 2004a	**0.41**	**5200** ±100 (2)	**18**	**1.7** ±0.4	This study
19	**6.7**	**16** ±2.5	Landais et al., 2004a	**0.42**	**1600**±150 (2)	**19**	**2.1**±0.4	This study
20	**6**	**11**±2.5	Landais et al., 2004a	**0.55**	**1200**±150(2)	**20**	**1.5**±0.4	This study
21	**4.2**	**12**±2.5	This study	**0.35**	**3600** ±300 (3)	**21**	**4.2** ±0.4	This study
22	**2**	**5**±2.5	This study	**0.40**	#	**22**	*	This study
23	**3.3**	**10**±2.5	Landais et al., 2006	**0.33**	**1400**±200 (3)	**23**	**2.4**±0.4	This study
23a	**3.8**				**300** ±60 (3)	**23a**	**1** ±0.4	This study
24	**5**	**16** ±2.5	Landais et al., 2006	**0.31**	**1700** ±100 (3)	**24**	**3** ±0.4	This study
25	**1.9**					**25**		

possibility of a large (greater than 1.6 kyr) error in interstadial duration unlikely and provides a firm basis to confidently analyse the interstadial structure and pacing of these events over MIS 5.

2.2 Past temperature reconstructions

The stable isotopic composition of precipitation at mid and high latitudes is related to local air temperature through the so-called spatial slope (Dansgaard, 1964) with an average of 0.67‰–δ^{18}O per °C in Greenland (Johnsen et al., 1989) and 0.75‰–δ^{18}O per °C in Antarctica (Lorius and Merlivat, 1977, Masson-Delmotte et al., 2008). This spatial slope, which results from air mass distillation processes, can be used as a surrogate for the temporal slope and may vary over time due to past changes in evaporation conditions or atmospheric transport. However, the ice isotopic composition as a tool for past temperature reconstructions (Dansgaard, 1964) has to be interpreted carefully. Indeed, the hypothesis of similar spatial and temporal slopes is only valid if

certain assumptions are satisfied, in particular those concerning the origin and seasonality of the precipitation (Jouzel et al., 1997).

In fact, past Greenland temperature reconstructions based on the spatial isotope-temperature slope have been challenged by alternative paleothermometry methods such as (i) the inversion of the borehole temperature profile (e.g. Dahl-Jensen et al., 1998; Cuffey and Clow, 1995; Johnsen et al., 1995) and (ii) the thermal diffusion of air in the firn arising during abrupt climate changes (Severinghaus et al., 1998). The quantitative interpretation of $\delta^{18}O_{ice}$ in term of temperature variations using this spatial relationship leads to a systematic underestimation of temperature changes (Jouzel, 1999). The amplitudes and shapes of temperature changes can be biased by past changes in precipitation seasonality (Fawcett et al., 1996; Krinner et al., 1997), changes in moisture sources during rapid events (Charles et al., 1994; Boyle, 1997; Masson-Delmotte et al., 2005a) and surface elevation (i.e. Vinther et al., 2009).

In contrast, available information suggests that reconstruction of local surface temperature in Antarctic ice cores using the present-day spatial relationship between isotopic composition of the snow and surface temperature ("isotopic thermometer") is correct, with a maximum associated uncertainty of 20% at the glacial-interglacial scale (Jouzel et al., 2003). As a consequence, the isotopic thermometer is commonly used to quantify past changes in temperature based on the stable isotopic composition measured in deep Antarctic ice cores (e.g. EPICA c.m., 2006; Jouzel et al., 2007). More recently, a modelling study dedicated to the stability of the temporal isotope-temperature slope suggests that the classical interpretation of the ice core stable isotopes on EDC may lead to an underestimation of past temperatures for periods warmer than present conditions (Sime et al., 2009).

2.2.1 Greenland temperature reconstruction

Measurements of the isotopic composition of nitrogen ($\delta^{15}N$) and/or argon ($\delta^{40}Ar$) from air trapped in ice cores provide independent quantitative reconstructions of abrupt local temperature changes (Severinghaus et al., 1998; Lang et al., 1999; Severinghaus and Brook, 1999; Landais et al., 2004a, b, c; Huber et al., 2006). Trapped-air $\delta^{15}N$ variations are only produced by firn isotopic fractionation due to gravitational settling and thermal diffusion since atmospheric $\delta^{15}N$ is constant over the past million years (Mariotti, 1983). The combined use of $\delta^{15}N$ and $\delta^{40}Ar$ data together with the modelling of physical processes (densification, temperature and gas diffusion) enable the estimation of abrupt surface temperature magnitudes with an accuracy of 2.5 °C (Landais et al., 2004a). Table 2 and Fig. 2 display a synthesis of all available $\delta^{15}N$-based temperature estimates for GIS amplitudes. Abrupt warmings of GIS 8 to GIS 17 vary between 8 to 15 °C (interval of uncertainty: +3/−6 °C; Huber et al., 2006). Over MIS 5, GIS 23 and 24 amplitudes

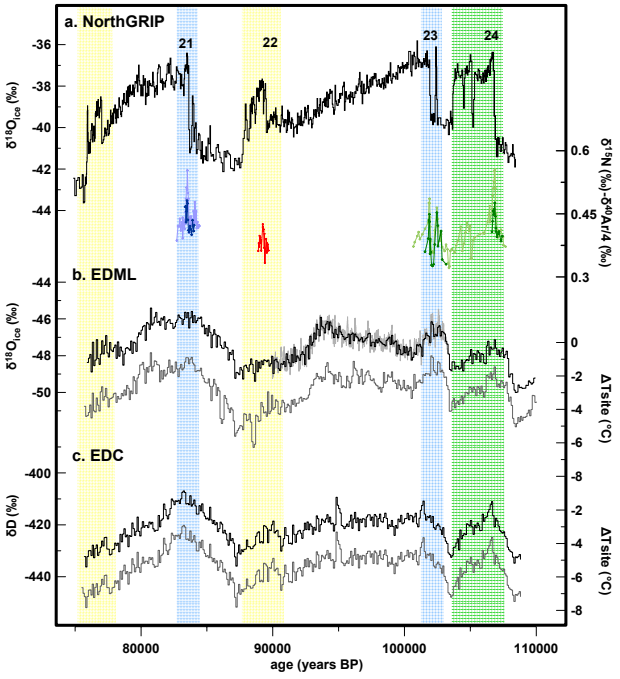

Fig. 3. Greenland-Antarctic isotopic records between 75 and 109 ka. **(a)** NorthGRIP $\delta^{18}O_{ice}$ records (black curve, NorthGRIP c.m., 2004), $\delta^{15}N$ measurements at the onset of GIS 21 (light blue curve, Capron et al., 2010), 22 (red curve, this study), 23 and 24 (light green curve, Landais et al., 2006) and $\delta^{40}Ar$ measurements at the onset of GIS 21 (dark blue curve, this study), 23 and 24 (dark green curve, Landais et al., 2006). **(b)** EDML $\delta^{18}O_{ice}$ plot of (i) bag sample data filtered on 100 yr time step (black curve; EPICA c.m., 2006) and (ii) high-resolution data (a 50 yr smoothing is performed on the 10 yr time step data, light grey curve, this study) and T_{site} reconstruction from Stenni et al. (2010, a 700 yr smoothing is performed on the 100 yr time step data, dark grey curve). **(c)** EDC $\delta^{18}O_{ice}$ plot of bag sample data filtered on 100 yr time step (black curve; Jouzel et al., 2007) and T_{site} reconstruction from Stenni et al. (2010; a 700 yr smoothing is performed on the 100 yr time step data, dark grey curve). Shaded bands mark the sub-millennial scale variability over MIS 5 GIS and their counterparts in Antarctica (Rebound-type events, yellow; Precursor-type events, blue; GIS 24, green).

show a warming of 10 °C ±2.5 °C and 16 °C ±2.5 °C, respectively (Landais et al., 2006). In the present paper, we complete the quantification of MIS 5 abrupt warming events based on published $\delta^{15}N$ measurements (Capron et al., 2010) with new $\delta^{40}Ar$ data for the onset of GIS 21 and new $\delta^{15}N$ measurements over GIS 22 (Fig. 3). Following the approach of Landais et al. (2004a), we find that the GIS 21 onset is marked by a warming of 11±2.5 °C while new high resolution gas measurements over GIS 22 reveal a weak $\delta^{15}N$ variation (0.063‰) corresponding to a maximum warming amplitude of 5 °C (Fig. 3).

Compared to the classical isotope-temperature relationship, the temporal slope between changes in δ^{18}O and in δ^{15}N-derived temperature at the onset of GIS events is systematically lower and varies from 0.29 to 0.55‰/ °C. Previous studies suggest an effect of obliquity and ice-sheet on the temporal $\delta^{18}O_{ice}$/temperature slope mainly via the seasonality of the precipitation and/or moisture source (Denton et al., 2005; Masson-Delmotte et al., 2005a; Flückiger et al., 2008). Here, we do not find any systematic relationship between the evolution of the temporal slope and the long term evolution of components such as ice sheet volume or orbital parameters. We suggest instead that the temporal slope and thus seasonality and/or moisture source change at the GIS scale.

Note that the amplitude of temperature change at the onset of the different GIS in NorthGRIP should not be used as a quantitative reference for Greenland climate. As an example, NorthGRIP and GISP2, only 325 km apart, present different temperature changes at the onset of GIS 19: 16 °C and 14 °C, respectively (Landais et al., 2004a; Landais, 2004). These regional differences are probably due to a more continental climate at NorthGRIP as has been suggested by the comparison of GRIP and NorthGRIP $\delta^{18}O_{ice}$ curves (NorthGRIP c.m., 2004). Indeed, it has been observed that the difference in $\delta^{18}O_{ice}$ between NorthGRIP and GISP2 is highly correlated with past continental ice volume reconstructions. This suggests that larger ice sheets enhance the remoteness of NorthGRIP from low latitudes air masses while Summit (GRIP/GISP2) is less affected by such continentality effect. Regional differences in moisture origin during the current interglacial period have also been identified in deuterium excess profiles (Masson-Delmotte et al., 2005b). Finally changes in ice sheet topography can also generate regional elevation changes impacting regional temperature at ice core sites (Vinther et al., 2009). However, these differences modulate the regional expressions of climate variability and do not prevent us to use the NorthGRIP $\delta^{18}O_{ice}$ profile to qualitatively characterise the relative amplitudes and shapes (Johnsen et al., 2001; NorthGRIP c.m., 2004).

2.2.2 Antarctica temperature reconstruction

Few studies have used so far the gas fractionation paleothermometry method on Antarctic records (Caillon et al., 2001; Taylor et al., 2004). Based on δ^{15}N and δ^{40}Ar data performed on the Vostok ice core, Caillon et al. (2001) estimate a temperature change at the MIS 5d/5c transition consistent within 20% of the classical interpretation of water stable isotope fluctuations. In general, the smoother shape of millennial scale temperature changes prevents the use of the isotopic composition of the air to infer local temperature change during AIM events using thermal diffusion. For Antarctic temperature reconstruction, we thus use the $\delta^{18}O_{ice}$-based method improved by using the deuterium excess data (d-excess=$\delta D - 8\times\delta^{18}O_{ice}$; Dansgaard, 1964) which allows us to correct for the changes in moisture source conditions (e.g. Stenni et al., 2001, 2010; Vimeux et al., 2002).

Here we use two different temperature reconstructions to characterize AIM warming amplitudes in East Antarctica. First, new high resolution and already published EDML $\delta^{18}O_{ice}$ and EDC δD profiles (Fig. 3) are corrected for global seawater isotopic composition (Bintanja et al., 2005) following Jouzel et al. (2003) and then converted to past temperatures using the observed spatial slope of $0.82\times\delta^{18}O_{ice}$ per °C for EDML (Oerter et al., 2004) and $6.04\times\delta$D per °C for EDC (Lorius and Merlivat, 1977; Masson Delmotte et al., 2008). These temperatures are corrected for elevation variations and changes in ice origin (upstream and elevation correction; for EDML: Huybrechts et al., 2007; for EDC: Parrenin et al., 2007b).

Secondly, we use the EDML and EDC temperature profiles derived using d-excess data recently published by Stenni et al. (2010). Based on isotopic profiles corrected for sea water isotopic composition and upstream effects, they estimate changes in source conditions and site temperature at both sites (Stenni et al., 2001; Masson-Delmotte et al., 2004). These site temperature reconstructions are expected to be more robust because they account for changes in evaporation conditions. However, for some rapid events, this "inverted" temperature is noisier and makes the beginning and the end of the warming more difficult to identify (Fig. 3; Stenni et al., 2010). Thus, both "classical" and "site" temperature reconstructions are used for EDC and EDML to identify AIM and associated warming amplitudes.

The AIM temperature change amplitudes are presented in Table 2. We estimate a maximum uncertainty of 0.4 °C based on (i) the warming amplitude difference between the two reconstructions and (ii) the determination of the minima and maxima for Antarctic temperature changes. The moisture correction does not have any major impact on AIM amplitudes nor on their shapes.

Note that Antarctic events with amplitudes of less than 1‰ (equivalent to 0.5 °C) remain delicate to interpret since corrections based on deuterium excess profiles add noise to the temperature reconstruction. We choose hereafter to discuss only small events that have a Greenland counterpart and to ignore the other small $\delta^{18}O_{ice}$ fluctuations.

3 Structure of MIS 5 abrupt climate variability

The exceptionally long duration of the GIS during MIS 5 reveals an additional variability within the classical GIS/GS succession. Three types of sub-millennial scale events are identified: (i) short-lived and sharp warming preceding GIS 21 and GIS 23, (ii) abrupt warming during the cooling phase of GIS 21 and (iii) abrupt cooling phases during GIS 24.

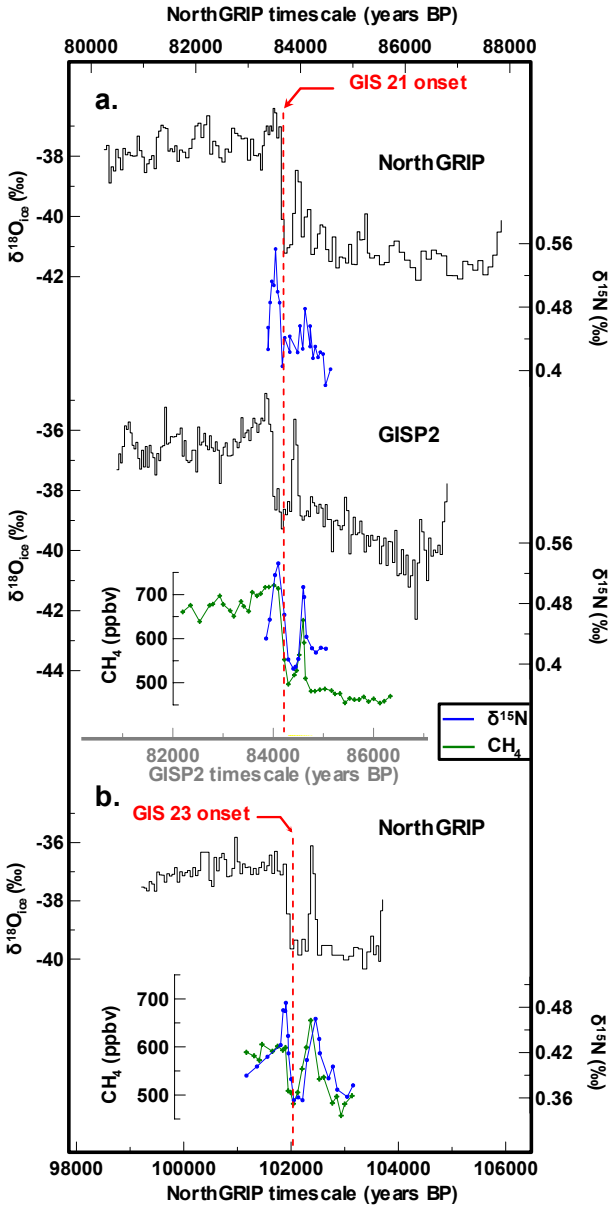

Fig. 4. **(a)** Short-lived sharp warming preceding GIS 21 recorded in NorthGRIP $\delta^{18}O_{ice}$ (NorthGRIP c.m., 2004) and $\delta^{15}N$ (Capron et al., 2010) and in GISP2 $\delta^{18}O_{ice}$ (Grootes and Stuiver, 1993), $\delta^{15}N$ and CH_4 (Grachev et al., 2007). **(b)** Short-lived sharp warming preceding GIS 23 recorded in NorthGRIP $\delta^{18}O_{ice}$ (NorthGRIP c.m., 2004) CH_4 (Capron et al., 2010) and $\delta^{15}N$ (Landais et al., 2006).

3.1 Precursor-type peak events

The NorthGRIP isotopic profile contains dramatic reversals in $\delta^{18}O_{ice}$ before the two longest GIS of the entire glacial period: GIS 21 and GIS 23 (Fig. 4). The first occurs within 200 yrs with a 2.2‰ variation in $\delta^{18}O_{ice}$. After a short (100 yrs) return to cold conditions, GIS 21 onset occurs with a 4.2‰ increase in $\delta^{18}O_{ice}$. Such a precursor-type structure is also visible before GIS 23 onset: the $\delta^{18}O_{ice}$ rises by 3.8‰ in 125 yrs at ∼102.5 ka and then drops by 3.6‰ in 100 yrs (hereafter, denoted as GIS 23b). The return to stadial conditions lasts ∼300 yrs before $\delta^{18}O_{ice}$ increases by 3‰ at the onset of GIS 23.

The occurrence of precursor events is confirmed by parallel $\delta^{18}O_{ice}$ variations measured in GRIP and GISP2 cores (Johnsen et al., 1992; Grootes and Stuiver, 1997; Grachev et al., 2007) and by their detection in high-resolution records of $\delta^{15}N$ data and CH_4. The precursor-type peak event leading GIS 23 exhibits a 200 ppbv variation in CH_4 and a 0.050‰ rapid increase in $\delta^{15}N$. The reversal prior to GIS 21 is weaker in the NorthGRIP $\delta^{18}O_{ice}$ profile (2.2‰) than GISP2 (3.4‰) whereas NorthGRIP $\delta^{15}N$ data over this reversal indicate a 0.08‰ variation in NorthGRIP comparable to the $\delta^{15}N$ variation of 0.09‰ measured in GISP2 (Grachev et al., 2007).

Note that these very short $\delta^{18}O_{ice}$ variations are not only visible during MIS 5. Indeed, the sequence of DO events 13 to 17 during MIS 3 is also extremely unstable with short temperature peaks of 200–400 yrs accompanied by fast shifts in CH_4 concentration (Blunier and Brook, 2001; Flückiger et al., 2004; Huber et al., 2006). This highlights that abrupt climatic variability over the glacial period is more complex than the millennial scale variations expressed by a GIS/GS succession.

3.2 Rebound-type events

At the end of the regular cooling phase of GIS 21, $\delta^{18}O_{ice}$ increases abruptly (∼2‰ in less than 100 yrs) 1.2 kyrs before the sharp return to stadial conditions (Fig. 5). The large scale imprint of the GIS 21 sub-event is detected through GISP2 high resolution CH_4 data (showing a 71 ppbv increase in 140 yrs; Grachev et al., 2009). This "rebound" pattern is identical in $\delta^{18}O_{ice}$ magnitude, duration and structure to GIS 22. GIS 23 ends with a smooth cooling making it impossible to clearly identify a GS 23 phase. Finally, the GIS 23-22 sequence of events shows exactly the same type of structure as the one observed over GIS 21.

Rebound-type events are not only restricted to MIS 5 as they are also occurring at the end of GIS 11, 12 and 16 (Fig. 5). GIS 13 also appears as a rebound event after the long GIS 14 without a clear GS 14. These rebound-type features are therefore recurrent over the glacial period and except for GIS 11 and GIS 12, are associated with the precursor-type events before GIS.

We also observe that rebound-type events are occurring at the end of a particularly long cooling phase during the GIS. Figure 5 highlights a linear link between the duration of GIS gradual cooling and the rebound event duration from multi-millennial (e.g. sequence of GIS 22-23 events and GIS 21) to few century timescales (e.g. GIS 11 and 16).

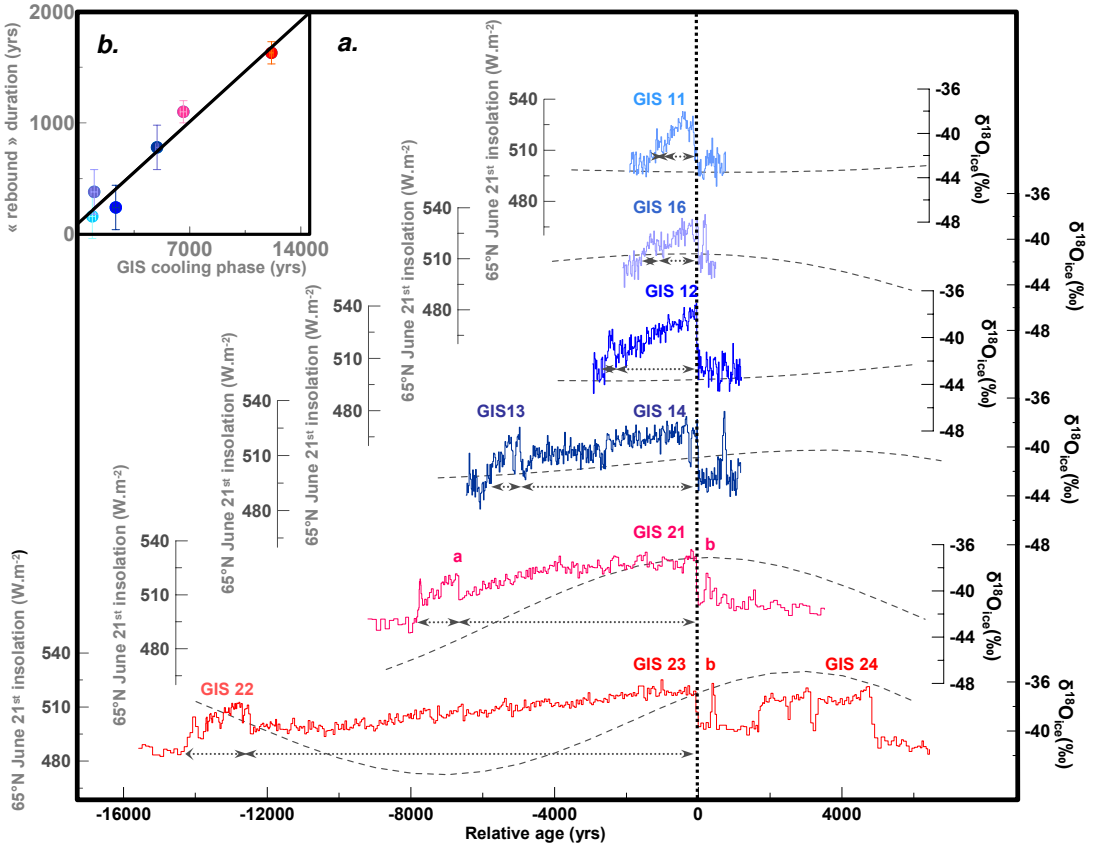

Fig. 5. **(a)** Sub-millennial scale climatic variability characterised by GIS preceded by precursor-type peak events, a rebound structure after GIS regular cooling phase and rapid cooling phases during GIS 24 (NorthGRIP c.m., 2004). 65° N insolation is superimposed to NorthGRIP isotopic records (Laskar et al., 2004). Dotted grey arrows indicate the gradual GIS cooling phase followed by the abrupt warming depicted as a "rebound" event. **(b)** Linear relationship between GIS cooling phase duration and associated duration of the rebound with associated uncertainties (R^2=0.95).

3.3 Abrupt coolings during GIS 24

GIS 24 presents a square wave structure beginning with an abrupt temperature warming of 16 °C (Landais et al., 2006) and ending 3.2 kyrs later by a sudden return to stadial conditions (Fig. 6). The warm phase is punctuated by rapid cold events i.e. the slow $\delta^{18}O_{ice}$ decrease is interrupted by a first drop of $\delta^{18}O_{ice}$ by 3‰ lasting 200 yrs before a return to interstadial $\delta^{18}O_{ice}$ level. A second cooling phase occurs 500 yrs later with a 2.5‰-$\delta^{18}O_{ice}$ decrease. Finally, a stable phase is observed with a duration of 500 yrs followed by the final return to stadial conditions in less than 200 yrs. The abrupt changes in $\delta^{18}O_{ice}$ are due to changes in surface temperature as confirmed by the associated two 0.04‰ drops in $\delta^{15}N$ coincident with $\delta^{18}O_{ice}$ abrupt variations (Fig. 6).

The first rapid cooling over GIS 24 appears to be accompanied by low latitudes counterparts as documented by a simultaneous drop in CH_4 concentration over 150–200 yrs. In addition, sub-millennial scale variations in $\delta^{18}O$ of O_2 have been identified during GIS 24 (Capron et al., 2010) reflecting significant changes of biosphere and hydrological cycles at these short timescales (Landais et al., 2010).

The very rapid climatic variability observed during the sequence GIS 23–24 with rapid events occurring in addition to the classical succession of GIS and GS, shares some similarities with the sequence of GIS/GS 15-17 that include 6 to 8 individual warming events depending on what one counts as a distinct warming event (Fig. 2).

The particularity of GIS 24 is that the first short cold spell occurs only ∼1380 yrs after the beginning of the GIS. The general picture of sub-millennial variability for this period is thus one of a cold event interrupting a long warm phase (GIS). By contrast, the later sub-millennial variability is better described in terms of brief warm events (GIS or precursor events) interrupting a long glacial phase (GS). With this view of a sharp cold spell interrupting a rather long warm phase, the sub-millennial variability of GIS 24 can only be compared with the 8.2 ka-event that occurred at the beginning of the Holocene (Alley et al., 1997; Leuenberger et

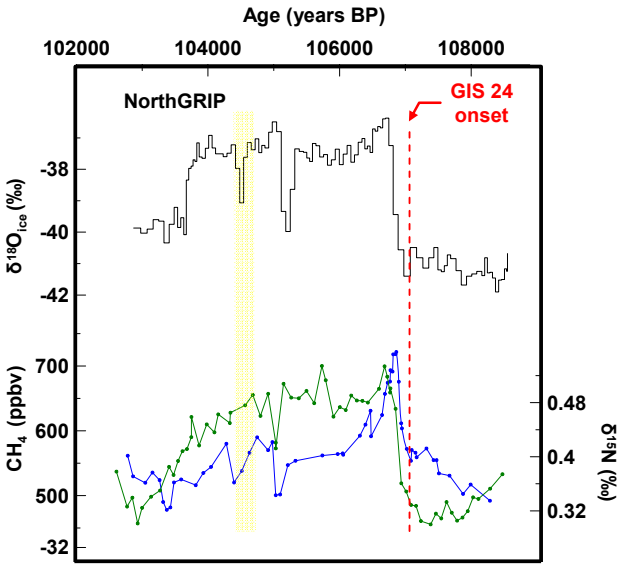

Fig. 6. GIS 24 recorded in NorthGRIP $\delta^{18}O_{ice}$ (black, NorthGRIP c.m., 2004), $\delta^{15}N$ (blue; Landais et al., 2006) and CH_4 (green, Capron et al., 2010). Red dotted line marks the synchronous onset of GIS 24 recorded in both ice and gas phases. Yellow shaded bands highlight abrupt coolings which interrupt the interstadial phase.

al., 1999; Kobashi et al., 2007; Thomas et al., 2007). These two cold events occur during two different periods of transition (glacial inception for the cold events of GIS 24, end of deglaciation for the 8.2 ka-event), but both at a time when ice sheets are relatively small. The AMOC during transitional periods is expected to be subject to rapid instabilities leading to sub-millennial variability because of strong modifications of the freshwater input linked to (i) freshwater discharge (von Grafenstein et al., 1998; Clarke et al., 2004) and/or (ii) enhanced precipitation (Khodri et al., 2001) and favoured by small ice sheets (Eisenman et al., 2009).

3.4 Antarctic sub-millennial scale variability

The new detailed $\delta^{18}O_{ice}$ measurements on the EDML ice core allow the identification of an Antarctic counterpart to the stadial phase between the precursor and GIS 23, as a 1‰ $\delta^{18}O_{ice}$ variation within a few decades (Fig. 3). This AIM shows a ∼1 °C temperature increase simultaneous to the cold Greenland phase lasting ∼400 yrs. As for the rapid variability during GIS 24, Antarctic $\delta^{18}O_{ice}$ and T_{site} reconstructions also exhibit sub-millennial counterparts. After reaching a relative temperature maximum corresponding to AIM 24, the general trend shows a regular decrease interrupted by a 1 kyr plateau that may correspond to the short cold spell occurring during GIS 24 (Fig. 3).

Note that we do not identify an Antarctic counterpart to the cold phase between the precursor and GIS 21 (Fig. 3). Two hypotheses could explain such a result: (i) a lack of resolution in the EDML $\delta^{18}O_{ice}$ profile (ii) the damping of Greenland temperature signals when transferred to Antarctica through the Southern Ocean.

4 Discussion

4.1 Millennial to sub-millennial scale GIS variability

The detailed analysis of the long GIS of MIS 5 provides evidence for sub-millennial scale variations during these phases. During GIS 21 and GIS 23, we depict a specific structure composed of a precursor-type warming event leading the GIS and a "rebound-type" abrupt event before the GIS abruptly ends. Such a structure is recurrent during MIS 3 at shorter timescales and Fig. 5 displays a linear relationship between the durations of the "rebound-type event" and of the preceding GIS regular cooling.

Inspired by the factors previously proposed for explaining the classical DO variability, we present here some of the possible mechanisms for favouring these additional sub-millennial scale features: (i) ice sheet size controlling iceberg discharges (MacAyeal, 1993) and the North Atlantic hydrological cycle (Eisenman et al, 2009) and (ii) 65° N insolation affecting temperature, seasonality, hydrological cycle and ice sheet growth in the high latitudes (e.g. Gallée et al., 1992; Crucifix and Loutre, 2002; Khodri et al., 2003; Flückiger et al., 2004). Note that these influences may also be enhanced through feedbacks. In particular, sea ice extent variations are often given as trigger (Wang and Mysak, 2006) or amplifiers (Li et al., 2005) of abrupt warming events.

We first discuss the link between the occurrence of the sub-millennial variability and the ice sheet volume. The length of the GIS displayed on Fig. 5 appears to be related to the mean sea level with the long GIS 23 and 21 being associated with the highest sea level while GIS 11, 12, 14 and 16 are associated with lower sea level during MIS 3 (Fig. 1). Such a link between the GIS length and sea level is expected from a simple Binge-Purge mechanism (MacAyeal, 1993): largest ice-sheets are expected to be easier to destabilize. However, such a Binge-Purge mechanism is unlikely to explain the existence of sub-millennial scale climatic events during sequences of events 21–24 and 15–17 since they occurs during relative ice sheet volume minima (Bintanja et al., 2005). A more plausible mechanism for these precursor events would be that the smaller ice sheets as observed during MIS 5 (equivalent to sea level of about 20 to 60 m above present sea level; Bintanja et al., 2005) are more vulnerable than large ice sheets observed during MIS 2-3-4 (sea level between 60 and 120 m above present sea level; Bintanja et al., 2005) to local radiative perturbations. If so, a strong 65° N summer insolation would lead to intermittent freshwater outputs and trigger fast changes in the AMOC intensity.

The influence of the Milankovitch insolation forcing on the sub-millennial variability can also be explored (Fig. 5). During MIS 5, the GIS 21 precursor-type event and GIS 24 are both in phase with two relative maxima in summertime insolation at 65° N. GIS 23 precursor-type event occurs during a relatively strong 65° N insolation and lags the preceding insolation maximum by only ∼2.5 kyrs (Fig. 5). During MIS 3, we again observe that precursor-type events GIS 14 and 16 are associated with secondary insolation maxima. On the contrary, GIS 11 and 12 are not preceded by a precursor and occur at a time without a marked anomaly in 65° N summer insolation. Our data therefore suggest a link between high 65° N insolation and the presence of a sub-millennial scale climatic variability in addition to the GS-GIS succession. This hypothesis also applies to the last deglaciation. Indeed, centennial-scale variations in the NorthGRIP $\delta^{18}O_{ice}$ profile are superimposed to the Bølling-Alleröd warm phase followed by the Younger-Dryas cooling (Björck et al., 1998) while the 65° N insolation during those events is equivalent to the one observed during the sequence of events 15–17.

Finally, rebound-type events tend to be associated with long GIS intervals characterized by a slow cooling. We speculate that the rebound at the end of the GIS could be explained by an enhancement of the AMOC. Indeed, a progressive cooling could increase sea ice formation and reduce precipitation amount/runoff, increasing salinity in the North Atlantic region.

4.2 The bipolar seesaw pattern

In the above discussion, we described rapid climatic variations over Greenland. Here, we use our common dating of Antarctic and Greenland ice cores to study the north-south millennial scale variability over the whole glacial period and test the general applicability of the conceptual thermal bipolar seesaw of Stocker and Johnsen (2003) especially over the new types of rapid events identified over MIS 5.

4.2.1 Millennial scale variations

Synchronised EDML and NorthGRIP isotopic records emphasized the close link between the amplitude of MIS 3 AIM warming and their concurrent stadial duration in Greenland (EPICA c.m., 2006). To complete this description we have added on Fig. 7 DO/AIM 2, 21, 23 and 24 using our MIS 5 timescale (EPICA c.m., 2006; Capron et al., 2010). Finally, DO/AIM events 18, 19 and 20 have also been added despite a lack of precise north-south common age scale over this period (Fig. 8).

EPICA c.m. (2006) reveal a linear dependency between the amplitude of the AIM warming and the duration of the concurrent stadial in the north for the shorter GIS and GS events during MIS 3. We observe that the linear fit established over MIS 3 also captures the characteristics of DO/AIM events 19, 20, 23 and 24 (Capron et al., 2010) but

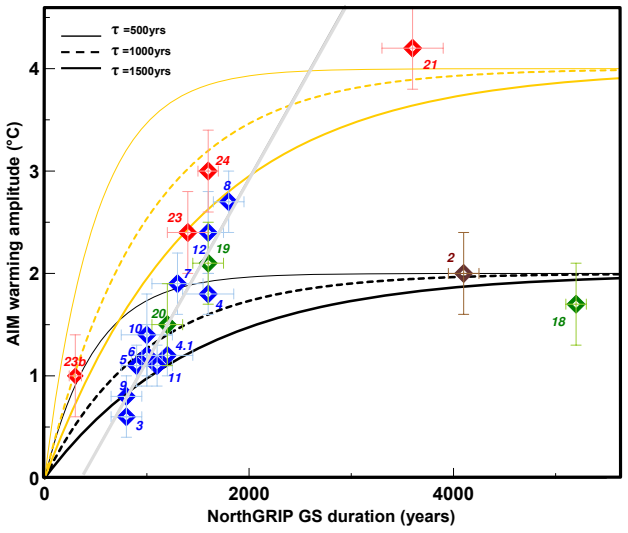

Fig. 7.

- Greenland stadial durations versus AIM warming amplitude over the last glacial period (MIS 5: red diamond, MIS 3: blue diamond, MIS 4: green diamond, MIS 2: brown diamond). Associated uncertainties are determined following EPICA c.m. (2006). Numbers indicate the corresponding AIM and DO events.
- Linear relationship for MIS 3 events established in EPICA c.m. (2006; light grey line).
- Evolutions of the relationship between Greenland stadial durations and AIM warming amplitudes inferred from the conceptual model for a thermal bipolar seesaw (Stocker and Johnsen, 2003; Eq. (1)) depending on (i) different characteristic timescales (500 yrs, thin curve; 1000 yrs, dotted thick curve; 1500 yrs, thick curve) and (ii) different values for T_N (−1/+1 amplitude, black curves; −2/+2 amplitude; yellow curves).

does not apply for DO/AIM events 2, 18 and 21. In fact, these DO exceptions are all preceded by exceptionally long cold periods in the NorthGRIP record. Exceptionally high temperature amplitudes would be expected from the linear regression as a GS duration of 4 kyr would correspond to an AIM warming of ∼5 °C, much stronger than the observed warming amplitude of the AIM 2, 18 and 21.

This shows that for extraordinarily long stadial durations the linear relationship between the stadial duration and the accompanying Antarctic warming amplitude is not longer valid. This feature is indeed expected from the bipolar seesaw concept (Stocker and Johnsen, 2003; EPICA c.m., 2006). Stocker and Johnsen (2003) predict that for long period of reduced AMOC (equivalent to GS duration in their model) a new equilibrium is reached and the Antarctic warming would eventually end. This type of situation could be relevant for the long DO/AIM 21, while DO/AIM events during MIS 3 may be too short for an equilibrium to be reached.

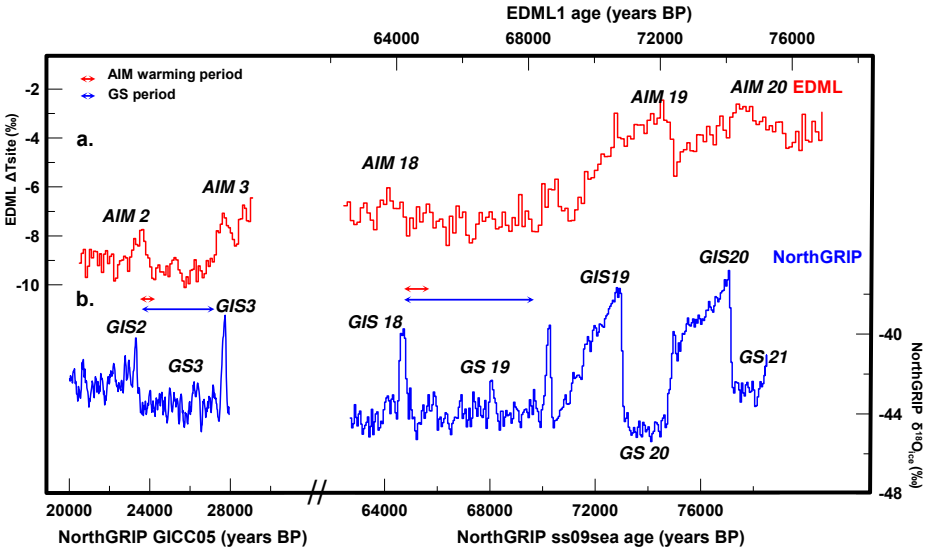

Fig. 8. **(a)** EDML ΔT_{site} (Stenni et al., 2010) over AIM 2 and the sequence of events from AIM 18 to AIM 20. All are presented on the EDML1 timescale (Ruth et al., 2007). **(b)** NorthGRIP $\delta^{18}O_{ice}$ over 20–28 ka: GICC05 timescale (Svensson et al., 2008); over 63–79 ka: ss09sea glaciological timescale (NorthGRIP c.m., 2004). Red Arrows represent warming durations of AIM 2 and AIM 18 and blue arrows represent GS 3 and GS 19 durations.

Here, we make a sensitivity test for the seesaw model in our case using the equation developed in Stocker and Johnsen (2003):

$$\Delta T_S(t) = -(1/\tau) \quad \int [T_N(t-t')e^{-t'/\tau}]dt' \qquad (1)$$

Where ΔT_S (t) represents the time-dependent temperature variation in the Southern Hemisphere, τ is the characteristic timescale of the heat reservoir in the Southern Hemisphere, T_N denotes the time-dependent temperature anomaly of the northern end of the bipolar seesaw. This equation predicts the southern temperature in response to climate signals in the North Atlantic region. The integral form associated with a characteristic time τ for the southern heat reservoir permits to describe the dampened temperature changes in the Southern Ocean in response to abrupt temperature changes in the North Atlantic. Following Stocker and Johnsen (2003), a value of -1 for T_N stands for a GS associated with an "off" mode of the AMOC. To model the abrupt GS/GIS transition associated with resumption of the AMOC, T_N changes from -1 to $+1$. A characteristic timescale τ of about 1000–1500 yrs has been determined to fit the Byrd temperature curve using the GRIP data as input.

On Fig. 7, we display ΔT_S simulations obtained with (i) changes in T_N of $-1/+1$ and $-2/+2$ and (ii) τ varying between 500 and 1500 yrs. The different results clearly illustrate a saturation level reached in the south when Greenland stadials are particularly long (more than 2000 yrs). The simulations with the largest T_N amplitude ($-2/+2$) permit to fit the AIM amplitude/NorthGRIP stadial duration for MIS 5 events, DO/AIM 8, 12 and 19. However, it is impossible to simulate the behaviours of all events of the glacial period with a fixed amplitude for T_N even with very large modifications of τ.

Our analysis suggests that larger amplitudes for T_N are needed to explain the Antarctic behaviour when ice sheets are smaller. However, one should be cautious with such interpretation since it is based on the hypothesis that the Antarctic temperature reflects the change in the Southern Ocean. This may not be systematically true. Indeed, AIM events can be linked to millennial scale temperature variations in the subantarctic surface waters (Pahnke et al., 2003) and a recent study based on a marine sediment core from the Southern Ocean shows that, while the amplitude of AIM 21 is clearly larger than the amplitude of AIM 23 in EPICA ice cores, the two respective Sea Surface temperature (SST) increases have the same magnitude (Govin et al., 2009). As a consequence, this change in Antarctic behaviour in regard to rapid variability of SST can be explained by variations in the heat transmission from Southern Ocean SST signals to the interior of Antarctic from one rapid event to the other. Such variations involve many further processes e.g. ocean-atmosphere heat fluxes, polar vortex position, sea-ice formation, ice sheet altitude that are in part related to ice sheets volume (Rind et al., 2001; Velinga and Wood, 2002).

The specific behaviour observed for AIM 2 and AIM 18 is not consistent with the same thermal bipolar seesaw pattern (Fig. 8). In fact, AIM 2 and AIM 18 warming periods are shorter than the corresponding northern stadial phases, ~700 yrs for each instead of GS durations of 4 kyrs and 5 kyrs, respectively. This highlights that Antarctic warming

does not systematically start with the beginning of a GS. Climate conditions of MIS 2 and MIS 4 were particularly cold as recorded in both marine (Bond et al., 1993; Chapman and Shackleton, 1998; de Abreu et al., 2003) and terrestrial records (e.g. Genty et al., 2003, 2006) and associated with vast ice sheets (Waelbroeck et al., 2002). Numerous studies have already shown that millennial scale climatic variability was reduced during MIS 2 and MIS 4 in relation with ice sheet volume (e.g. McManus et al., 1999; Schulz et al., 2002; Wang and Mysak, 2006; NorthGRIP c.m., 2004; Margari et al., 2010). Our study suggests that the bipolar seesaw was also affected during these cold periods.

Several explanations can be proposed for this particular see-saw pattern: a first possibility could be that the expansion of the Antarctic ice sheet and sea-ice during these two particular periods would increase the isolation of Antarctica and therefore decrease the heat received by the continent from the Southern Ocean (Levermann et al., 2007). A second possibility is linked to the AMOC activity. Marine records have revealed that the AMOC structure and dynamic was different over MIS 4 and end of MIS 2 compared to MIS 3 and MIS 5 in both hemispheres (e.g. Gherardi et al., 2009; Govin et al., 2009; Guihou, 2009). This particular configuration may have lead to an AMOC not strictly in an "off" mode during the whole GS. The AMOC might have been significantly reduced for the entire cold period in the north during GS 3 and 19 but could have collapsed just a few hundred years before the end of the cold phase.

4.2.2 Sub-millennial scale variations

In Sect. 3.3, we have shown that an Antarctic counterpart exists for the sub-millennial variability recorded in Greenland. This is especially obvious for GIS 23b. When displaying the amplitude of the Antarctic warming against the duration in the Greenland cold phase (Fig. 7), we find that it is consistent with the curve representing MIS 5 events. This result highlights that even at sub-millennial scale, the bipolar seesaw model of Stocker and Johnsen (2003) is still valid.

Using an amplitude of ± 2 for T_N and a characteristic timescale of 1000 yrs for the heat reservoir turned out to be the best way to describe MIS 5 rapid events. We thus apply this tuning for generating T_S curves corresponding to the sub-millennial scale structures highlighted during MIS 5 (GIS 24 and 23).

When we use a stadial duration of $\sim$1150 yr with a $\sim$300 yr cold phase between the precursor type peak event and the main abrupt warming, the conceptual model reproduces the same singular structure in the Antarctic counterpart as observed in the data (Fig. 9).

We then construct a time-series of T_N corresponding to GIS 24 characterised by an abrupt cooling phase lasting 200 yr (Fig. 10). We observe a plateau interrupting the regular cooling phase after AIM 24 as depicted by the

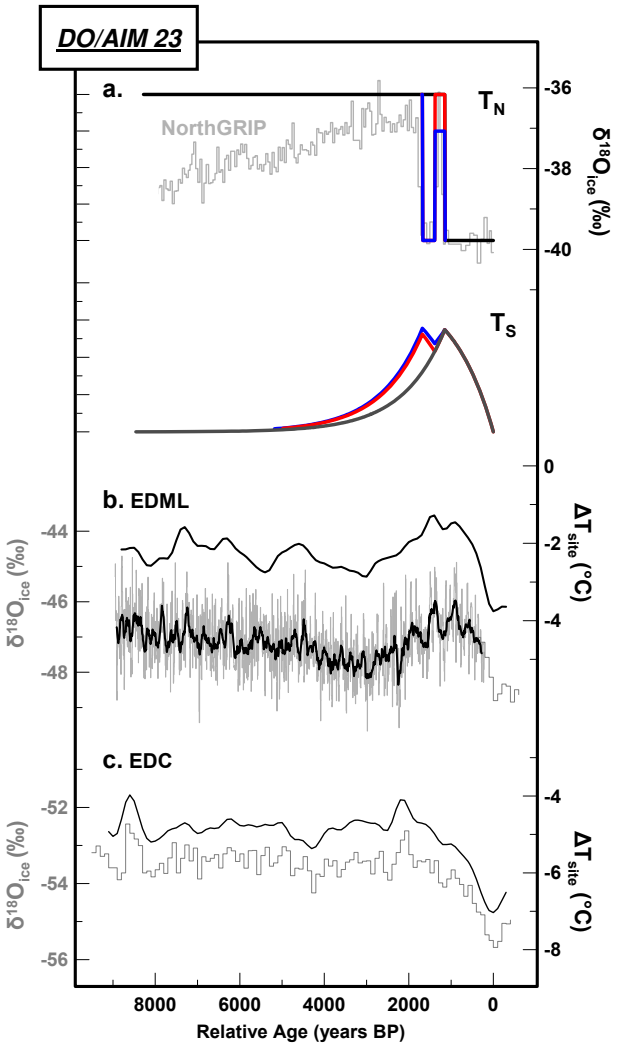

Fig. 9. **(a)** North-south time-series generated through the conceptual thermal bipolar seesaw model (Stocker and Johnsen, 2003) for GIS 23 associated with the precursor event. Different configurations of the northern perturbation (T_N, superimposed to NorthGRIP $\delta^{18}O_{ice}$ data) are used to simulate the response of the Southern Hemisphere (T_S). One configuration (dark grey curve) represents the evolution of T_S in response to T_N that corresponds to an "on-off" signal with 1150 years off (amplitude -2) and 7340 years on (amplitude +2). Two additional configurations (blue and red curves) are superimposed to illustrate the thermal bipolar seesaw pattern at a sub-millennial scale. T_N is structured as an "on-off" signal with 1150 years off (amplitude -2), 240 years on (red curve, amplitude +2; blue curve, amplitude +1), 300 years off (amplitude -2) and 6800 years on (amplitude +2). **(b)** EDML high-resolution data (a 50 yr smoothing is performed on the 10 yr time step data, light grey curve, this study) and T_{site} reconstruction from Stenni et al. (2010, a 700 yr smoothing is performed on the 100 yr time step data, dark grey curve). **(c)** EDC $\delta^{18}O_{ice}$ (grey step curve) and T_{site} reconstruction (dark grey curve; Stenni et al., 2010).

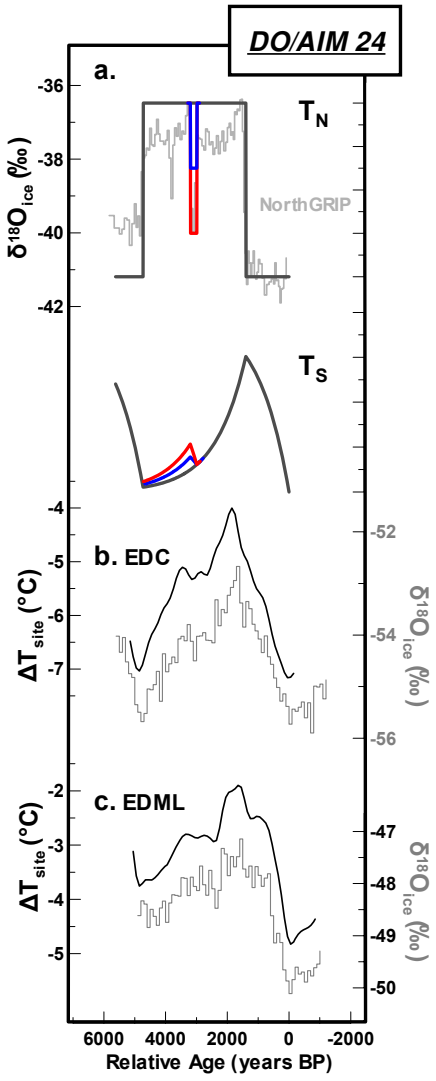

Fig. 10. **(a)** North-south time-series generated through the conceptual thermal bipolar seesaw model (Stocker and Johnsen, 2003) for GIS 24. Different configurations of the northern perturbation (T_N, superimposed to NorthGRIP $\delta^{18}O_{ice}$ data) are used to simulate the response of the Southern Hemisphere (T_S). One configuration (dark grey curve) represents the response of the Southern Hemisphere (T_S) to T_N that corresponds to an "on-off" signal with 1400 years off (amplitude −2), 3330 years on (amplitude +2) and 700 years off (amplitude −2). Two other configurations (blue and red curves) are superimposed to illustrate the thermal bipolar seesaw pattern at a sub-millennial scale. T_N is structured as an "on-off" signal with 1400 years off (amplitude −2), 1590 years on (amplitude +2), 200 years off (red curve, amplitude −1; blue curve amplitude 0), 1530 years on (amplitude +2) and 700 years off (amplitude −2). **(b)** EDC $\delta^{18}O_{ice}$ (Jouzel et al., 2007) and T_{site} reconstruction (Stenni et al., 2010). **(c)** EDML $\delta^{18}O_{ice}$ (EPICA c.m., 2006) and T_{site} reconstruction (Stenni et al., 2010).

temperature reconstruction of both EPICA cores. Results obtained on both events 23 and 24 emphasize the ability of the model tuned on MIS 5 to explain the sub-millennial scale variability depicted in Antarctic isotopic records.

5 Summary and perspectives

In this paper, we present the most recent and accurate Greenland–Antarctica common dating over the last 123 ka using the NorthGRIP and EPICA ice cores. We used new and published measurements of air isotopic composition in the NorthGRIP ice core to compare the local amplitudes of temperature changes for GIS of MIS 5 and MIS 3. A study of the $\delta^{18}O_{ice}$/temperature slope at the onset of each rapid event shows a strong variability from one GIS event to another but no systematic difference between MIS 3 and MIS 5 events. For Antarctica, we have combined new and published water isotope records to present detailed temperature reconstructions of Antarctic temperature based on EPICA isotopic records.

NorthGRIP records enable us to depict the sub-millennial scale variability during the GIS of MIS 5 and thus, to highlight new type of features (GIS 21, 23) observed also during MIS 3 (GIS 11, 12, 13–14, 16). These new patterns appear as (i) precursor-type events prior to the onset of GIS (ii) rebound events at the end of GIS and (iii) centennial-scale cooling during the long and warm GIS 24. In addition to the internal forcing of ice-sheets on the climatic evolution during these events, we have proposed the external influence of the summertime insolation at 65° N. Disentangling the main processes leading to these sub-millennial scale structures (ice-sheet, insolation, sea-ice, and hydrological cycle forcing) will require dedicated modelling studies. Through our results, we assume that orbital-scale variations play a role in rapid climate change but, also, the millennial-scale variability may hold clues to the long term climatic changes (i.e. Weirauch et al., 2008; Wolff et al., 2009b).

Comparing Antarctic and Greenland behaviour over the succession of AIM/DO back to MIS 5 provides a more complete description of the bipolar seesaw pattern. As expect from the bipolar seesaw concept, a linear relationship between AIM amplitude and preceding GS duration only holds for shorter events, while for extraordinary long GS a new heat flux equilibrium between the Northern and Southern Hemisphere is obtained (EPICA c.m., 2006, Stocker and Johnsen, 2003) and the Southern Ocean warming ceases. The conceptual model of Stocker and Johnsen (2003) for a thermal bipolar seesaw is able to represent most of the variability of the north-south relationship depicted in Greenland and Antarctic isotopic records, even at sub-millennial timescale. However, it is not able to depict the delay of Antarctic warming after the beginning of the GS during the periods associated with large ice sheets (i.e. during MIS 2 and the end of

MIS 4). It shows that Greenland ice core temperature proxy records cannot be taken as direct proxy for AMOC changes as suggested from the conceptual model.

To go beyond our description and the conceptual model of Stocker and Johnsen (2003), the new types of DO events identified during MIS 5 should be studied with more complex models (e.g. Ganopolski and Rahmstorf, 2001; Knutti et al., 2004). This would allow quantification of the influence of insolation, ice-sheet volume, sea-ice and hydrological cycle on sub-millennial-scale variability (precursor and rebound events). This should provide also a better understanding of the response of Antarctica to these types of events.

Acknowledgements. We are grateful to M. Crucifix, H. Fisher, A. Govin and D. Roche for discussions and their helpful comments on the manuscript. We thank Jeff Severinghaus and an anonymous reviewer for their constructive comments that help to improve the manuscript. This work was supported by ANR PICC and ANR NEEM and is a contribution to the European Project for Ice Coring in Antarctica (EPICA), a joint European Science, Foundation/European Commission scientific programme, funded by the EU (EPICA-MIS) and by national contributions from Belgium, Denmark, France, Germany, Italy, The Netherlands, Norway, Sweden, Switzerland and the United Kingdom. The main logistic was provided by IPEV and PNRA (at Dome C) and AWI (at Dronning Maud Land). This work is a contribution to the North Greenland Ice Core Project (NGRIP) directed and organized by the Department of Geophysics at the Niels Bohr Institute for Astronomy, Physics and Geophysics, University of Copenhagen. It is supported by funding agencies in Denmark (SNF), Belgium (FNRS-CFB), France (IPEV and INSU/CNRS), Germany (AWI), Iceland (RannIs), Japan (MEXT), Sweden (SPRS), Switzerland (SNF) and the USA (NSF, Office of Polar Programs). This is EPICA publication n°268 and LSCE publication n°4208.

Edited by: E. Wolff

The publication of this article is financed by CNRS-INSU.

References

Alley, R. B., Mayewski, P. A., Sowers, T., Stuiver, M., Taylor, K. C., and Clark, P. U.: Holocene climatic instability: a prominent, widespread event 8200 years ago, Geology 25, 483–486, 1997.

Barker, S., Diz, P., Jautravers, M. J., Pike, J., Knorr, G., Hall, I. R., and Broecker, W. S.: Interhemispheric Atlantic seesaw response during the last deglaciation, Nature 457, 1097–1102, 2009.

Bender, M., Sowers, T., Dickson, M. L., Orchardo, J., Grootes, P., Mayewski, P. A., and Meese, D. A.: Climate Correlations between Greenland and Antarctica during the Past 100 000 Years, Nature 372, 663–666, 1994.

Bintanja, R., van de Wal, R. S. W., and Oerlemans, J.: Modelled atmospheric temperatures and global sea levels over the past million years, Nature, 437, 125–128, 2005.

Björck, S., Walker, M. J. C., Cwynar, L. C., Johnsen, S., Knudsen, K. L., Lowe, J. J., and Wohlfarth, B.: An event stratigraphy for the Last Termination in the north Atlantic region based on the Greenland ice-core record: a proposal by the INTIMATE group, J. Quaternary Sci., 13, 283–292, 1998.

Blunier, T., Chappellaz, J., Schwander, J., Dällenbach, A., Stauffer, B., Stocker, T. F., Raynaud, D., Jouzel, J., Clausen, H. B., Hammer, C. U., and Johnsen, S. J.: Asynchrony of Antarctic and Greenland climate change during the last glacial period, Nature 394, 739–743, 1998.

Blunier, T. and Brook, E. J.: Timing of millennial-scale climate change in Antarctica and Greenland during the last glacial period, Science, 291, 109–112, 2001.

Blunier, T., Spahni, R., Barnola, J.-M., Chappellaz, J., Loulergue, L., and Schwander, J.: Synchronization of ice core records via atmospheric gases, Clim. Past, 3, 325–330, doi:10.5194/cp-3-325-2007, 2007.

Bond, G., Heinrich, H., Huon, H., Broecker, W. S., Labeyrie, L., Andrews, J., McManus, J., Clasen, S., Tedesco, K., Jantschik, R., and Simet, C.: Evidence for massive discharges of icebergs into the glacial Northern Atlantic, Nature, 360, 245–249, 1992.

Bond, G., Broecker, W., Johnsen, S., McManus, J., Labeyrie L., Jouzel J., and Bonani, G.: Correlations between climate records from North Atlantic sediments and Greenland ice, Nature 365, 143–147, 1993.

Boyle, E. A.: Cool tropical temperatures shift the global δ^{18}O-T relationship: An explanation for the ice core δ^{18}O borehole thermometry conflict?, Geophys. Res. Lett., 24, 273–276, 1997.

Brauer, A., Allen, J. R. M., Mingram, J., Dulski, P., Wulf, S., and Huntley, B.: Evidence for interglacial chronology and environmental change from Southern Europe, PNAS 104/2, 450–455, 2007.

Braun, H., Ditlevsen, P., and Chialvo, D. R.: Solar forced Dansgaard-Oeschger events and their phase relation with solar proxies, Geophys. Res. Lett., 35, L06703, doi:10.1029/2008GL033414, 2008.

Broecker, W. S.: Paleocean circulation during the last deglaciation: A bipolar seesaw?, Paleoceanography 13, 119–121, 1998.

Broecker, W. S.: Does the Trigger for Abrupt Climate Change Reside in the Ocean or in the Atmosphere?, Science, 300, 1519–1522, 2003.

Broecker, W. S., Bond, G., Klas, M., Bonani, G., and Wolfli, W.: A salt oscillator in the glacial Atlantic? The Concept, Paleoceanography, 5, 469–477, 1990.

Caillon, N., Severinghaus, J. P., Jouzel, J., Barnola, J.-M., Kang, J., and Lipenkov, V. Y.: Timing of atmospheric CO_2 and Antarctic temperature changes across termination III, Science, 299, 1728–1731, 2001.

Capron, E., Landais, A., Lemieux-Dudon, B., Schilt A., Masson-Delmotte, V., Buiron, D., Chappellaz, J., Dahl-Jensen, D., Johnsen, S. J., Leuenberger, M., Loulergue, L., and Oerter, H.: Synchronising EDML and NorthGRIP ice cores using δ^{18}O

of atmospheric oxygen ($\delta^{18}O_{atm}$) and CH_4 measurements over MIS 5 (80–123 kyr), Quaternary Sci. Rev., 29, 222–234, 2010.

Chapman, M. R., and Shackleton, N. J.: Millennial-scale fluctuations in North Atlantic heat flux during the last 150,000 years, Earth Planet Sc. Lett., 159, 57–70, 1998.

Chappellaz, J., Blunier, T., Raynaud, D., Barnola, J.-M., Schwander, J., and Stauffer, B.: Synchronous Changes in Atmospheric CH_4 and Greenland Climate between 40 kyr and 8 kyr BP, Nature, 366, 443–445, 1993.

Charles, C., Rind, D., Jouzel, J., Koster, R., and Fairbanks, R.: Glacial-interglacial changes in moisture sources for Greenland: influences on the ice core record of climate, Science, 261, 508–511, 1994.

Clarke, G. K. C., Leverington, D. W., Teller, J. T., and Dyke, A. S.: Paleohydraulics of the last outburst flood from glacial Lake Agassiz and the 8200 yrs BP cold event, Quaternary Sci. Rev., 23, 389–407, 2004.

Cortijo, E., Duplessy, J. C., Labeyrie, L., Leclaire, H., Duprat, J., and van Weering, T. C. E.: Eemian cooling in the Norwegian Sea and North Atlantic ocean preceding continental ice-sheet growth, Nature, 372, 446–449, 1994.

Crucifix, M. and Loutre, M. F.: Transient simulations over the last interglacial period (126–115 kyr BP): feedback and forcing analysis, Clim. Dynam., 19, 417–433, 2002.

Cuffey, K. M. and Clow, G. D.: Temperature, accumulation and ice sheet elevation in central Greenland through the last deglacial transition, J. Geophys. Res., 102(C12), 26383–26396, 1995.

Dahl-Jensen, D., Mosegaard, K., Gundestrup, N., Clow, G. D., Johnsen, S. J., Hansen, A. W., and Balling, N.: Past temperatures directly from the Greenland ice sheet, Science, 282, 268–271, 1998.

Dahl-Jensen, D., Gundestrup, N., Gogineni, P., and Miller, H.: Basal melt at NorthGRIP modeled from borehole, ice-core and radio-echo sounder observations, Ann. Glaciol., 37, 207–212, 2003.

Dansgaard, W.: Stable isotopes in precipitation, Tellus 16, 436–468, 1964.

Dansgaard, W., Johnsen, S. J., Clausen, H. B., Dahl-Jensen, D., Gunderstrup, N. S., Hammer, C. U., Steffensen, J. P., Sveinbjörnsdottir, A., Jouzel, J., and Bond, G.: Evidence for general instability of past climate from a 250-kyr ice-core record, Nature, 364, 218–220, 1993.

de Abreu, L., Shackleton, N. J., Schönfeld, J., Hall , M., and Chapman, M. R.: Millennial-scale oceanic climate variability of the Western Iberian margin during the last glacial periods, Mar. Geol., 196, 1–20, 2003.

Denton, G. H., Alley, R. B., Comer, G. C., and Broecker, W. S.: The role of seasonality in abrupt climate change George, Quaternary Sci. Rev., 24, 1159–1182, 2005.

Ditlevsen, P. D., Kristensen, M. S., and Andersen, K. K.: The recurrence time of Dansgaard-Oeschger events and limits on the possible periodic component, J. Climate 18, 2594–2603, 2005.

Ditlevsen, P. D., Andersen, K. K., and Svensson, A.: The DO-climate events are probably noise induced: statistical investigation of the claimed 1470 years cycle, Clim. Past, 3, 129–134, doi:10.5194/cp-3-129-2007, 2007.

Eisenman, I., Bitz, C. M., and Tziperman, E.: Rain driven by receding ice sheets as a cause of past climate change, Paleoceanography, 24, PA4209, doi:10.1029/2009PA001778, 2009.

EPICA-community-members: One-to-one coupling of glacial climate variability in Greenland and Antarctica, Nature, 444, 195–198, 2006.

Eynaud, F., Turon, J.-L., Sanchez-Goni, M.-F., and Gendreau, S.: Dinoflagellate cyst evidence of 'Heinrich-like events' off Portugal during the Marine Isotopic Stage 5, Mar. Micropaleontol. 40, 9–21, 2000.

Fairbanks, R. G., Mortlock, R. A., Chiu, T.-C., Cao, L., Kaplan, A., Guilderson, T. P., Fairbanks, T. W., and Bloom, A. L.: Marine radiocarbon calibration curve spanning 10 000 to 50 000 years B.P. based on Paired $^{230}Th/^{234}U/^{238}U$ and ^{14}C dates on pristine corals, Quaternary Sci. Rev., 24, 1781–1796, 2005.

Fawcett, P. J., Agustdottir, A. M., Alley, R. B., and Shuman, C. A.: The younger dryas termination and North Atlantic deepwater formation: insights from climate model simulations and greenland ice data, Paleooceanography, 12, 23–38, 1996.

Fleitmann, D., Cheng, H., Badertscher, S., Edwards, R. L., Mudelsee, M., Göktürk O. M., Fankhauser, A., Pickering, R., C. Raible, C. C., Matter, A., Kramers, J., and Tüysüz, O.: Timing and climatic impact of Greenland interstadials recorded in stalagmites from northern Turkey, Geophys. Res. Lett., 36, L19707, doi:10.1029/2009GL040050, 2009.

Flückiger, J., Blunier, T., Stauffer, B., Chappellaz, J., Spahni, R., Kawamura, K., Schwander, J., Stocker, T. F., and Dahl-Jensen, D.: N_2O and CH_4 variations during the last glacial epoch: Insight into global processes, Global. Biogechem. Cy., 18, doi:10.1029/2003GB002122, 2004.

Flückiger, J., Knutti, R., White, J. W. C., and Renssen, H.: Modeled seasonality of glacial abrupt climate events, Clim. Dynam. 31, 633–645, 2008.

Friedrich, T., Timmermann, A., Timm, O., Mouchet, A., and Roche, D. M.: Orbital modulation of millennial-scale climate variability in an earth system model of intermediate complexity, Clim. Past Discuss., 5, 2019–2051, doi:10.5194/cpd-5-2019-2009, 2009.

Gallée, H., van Ypersele, J. P., Fichefet, T., Marsiat, I., Tricot, C., and Berger, A.: Simulation of the last glacial cycle by a coupled, sectorially averaged climate-ice sheet model. Part II : Response to insolation and CO variation, J. Geophys. Res., 97, 15713–15740, 1992.

Ganopolski, A. and Rahmstorf, S.: Rapid changes of glacial climate simulated in a coupled climate model, Nature, 409, 153–158, 2001.

Genty, D., Blamart, D., Ouahdl, R., Gillmour, M., Baker, A., Jouzel, J., and Van-Exter, S.: Precise dating of Dansgaard Oeschger climate oscillations in western Europe from stalagmite data, Nature, 421, 833–837, 2003.

Genty, D., Blamart, D., Ghalebb, B., Plagnes, V., Causse, C., Bakalowicz, M., Zouarif, B., Chkir, N., Hellstrom, J., Wainer, K., and Bourges, F.: Timing and dynamics of the last deglaciation from European and North African $\delta^{13}C$ stalagmite profiles-comparison with Chinese and South Hemisphere stalagmites, Quaternary Sci. Rev., 25, 2118–2142, 2006.

Gherardi, J. M., Labeyrie, L., Nave S., Francois, R., McManus, J. F., and Cortijo, E.: Glacial-interglacial circulation changes inferred from $^{231}Pa/^{230}Th$ sedimentary record in the North Atlantic region, Paleoceanography, 24, PA2204, doi:10.1029/2008PA001696, 2009.

Govin, A., Michel, E., Labeyrie, L., Waelbroeck, C., Dewilde, F., and Jansen, E.: Evidence for northward expansion of

Antarctic Bottom Water mass in the Southern Ocean during the last glacial inception, Paleoceanography, 24, PA1202, doi:10.1029/2008PA001603, 2009.

Grachev, A. M., Brook, E. J., and Severinghaus, J. P.: Abrupt changes in atmospheric methane at the MIS5b-5a transition, Geophys. Res. Lett. 34, doi:10.1029/2007GL029799, L207703, 2007.

Grachev, A. M., Brook, E. J., Severinghaus, J. P., and Pisias, N. G.: Relative Timing and Variability of Atmospheric Methane and GISP2 Oxygen Isotopes Between 68 and 86 ka., Global. Biogechem. Cy., 23, GB2009, doi:10.1029/2008GB003330, 2009.

GRIP-members: Climate instability during the last interglacial period recorded in the GRIP ice core, Nature, 364, 203–208, 1993.

Grootes, P. M., Stuiver, M., White, J. W. C., Johnsen, S. J., and Jouzel, J.: Comparison of the oxygen isotope records from the GISP2 and GRIP Greenland ice cores, Nature, 366, 552–554, 1993.

Grootes, P. M., and Stuiver, M.: Oxygen 18/16 variability in Greenland snow and ice with 10^{-3}– to 10^{5}-year time resolution, J. Geophys. Res., 102, 26 455–26 470, 1997.

Guihou, A.: Reconstitutions des variations de la dynamique de la circulation méridienne Atlantique lors de la dernière entrée en glaciation par le rapport (^{231}Pa/^{230}Th) des sédiments marins, Thèse de doctorat de l'Université de Versailles St Quentin en Yvelines, 160 pp., 2009.

Hendy, I. L. and Kennett, J. P.: Latest Quaternary North Pacific surface-water responses imply atmosphere-driven climate instability, Geology, 27, 291–294, 1999.

Heusser, L. and Oppo, D. W.: Millennial- and orbital-scale climate variability in southeastern United States and in the subtropical Atlantic during Marine Isotope Strage 5: evidence from pollen and isotopes in ODP Site 1059, Earth Planet. Sc. Lett., 214, 483–490, 2003.

Huber, C., Leuenberger, M., Spahni, R., Flückiger, J., Schwander, J., Stocker, T. F., Johnsen, S., Landais, A., and Jouzel, J.: Isotope calibrated Greenland temperature record over Marine Isotope Stage 3 and its relation to CH_4, Earth Planet. Sc. Lett. 243, 504–519, 2006.

Huybrechts, P., Rybak, O., Pattyn, F., Ruth, U., and Steinhage, D.: Ice thinning, upstream advection, and non-climatic biases for the upper 89‰of the EDML ice core from a nested model of the Antarctic ice sheet, Clim. Past, 3, 577–589, doi:10.5194/cp-3-577-2007, 2007.

Johnsen, S., Dahl-Jensen, D., Dansgaard, W., and Gundestrup, N.: Greenland palaeotemperatures derived from GRIP bore hole temperature and ice core isotope profiles, Tellus, 47B, 624–629, 1995.

Johnsen, S. J. Dansgaard, W., and White, J. W. C.: The origin of Arctic precipitation under present and glacial conditions, Tellus, 41, 452–469, 1989.

Johnsen, S. J., Clausen, H. B., Dansgaard, W., Fuhrer, K., Gundestrup, N., Hammer, C. U., Iversen, P., Jouzel, J., Stauffer, B., and Steffensen, J. P.: Irregular glacial interstadials recorded in a new Greenland ice core, Nature, 359, 311–313, 1992.

Johnsen, S. J., Dahl-Jensen, D., Gundestrup, N., Steffensen, J. P., Henrick, B., Clausen, H. B., Miller, H., Masson-Delmotte, V., Sveinbjornsdottir, A., and White, J. W. C.: Oxygen isotope and palaeotemperature records from six Greenland ice-core stations: Camp Century, Dye-3, GRIP, GISP2, Renland and NorthGRIP, J. Quaternary Sci., 16, 299–307, 2001.

Jouzel, J., Alley, R. B., Cuffey, K. M., Dansgaard, W., Grootes, P., Hoffmann, G., Johnsen, S. J., Koster, R. D., Peel, D., Shuman, C. A., Stievenard, M., Stuiver, M., and White, J.: Validity of the temperature reconstruction from ice cores, J. Geophys. Res., 102, 26 471–26 487, 1997.

Jouzel, J.: Calibrating the isotopic paleothermometer, Science, 286, 910–911, 1999.

Jouzel, J., Vimeux, F., Caillon, N., Delaygue, G., Hoffmann, G., Masson-Delmotte, V., and Parrenin, F.: Magnitude of the isotope/temperature scaling for interpretation of central Antarctic ice cores, J. Geophys. Res., 108, 1029–1046, 2003.

Jouzel, J., Masson-Delmotte, V., Cattani, O., Dreyfus, G., Falourd, S., Hoffmann, G., Minster, B., Nouet, J., Barnola, J.-M., Fisher, H., Gallet, J.-C., Johnsen, S., Leuenberger, M., Loulergue, L., Luethi, D., Oerter, H., Parrenin, F., Raisbeck, G., Raynaud, D., Schilt, A., Schwander, J., Selmo, J., Souchez, R., Spahni, R., Stauffer, B., Steffensen, J. P., Stenni, B., Stocker, T. F., Tison, J.-L., Werner, M., and Wolff, E. W.: Orbital and millennial Antarctic climate variability over the past 800 000 years, Science, 317, 793–796, 2007.

Kageyama, M., Mignot, J., Swingedouw, D., Marzin, C., Alkama, R., and Marti, O.: Glacial climate sensitivity to different states of the Atlantic Meridional Overturning Circulation: results from the IPSL model, Clim. Past, 5, 551–570, doi:10.5194/cp-5-551-2009, 2009.

Khodri, M., Leclainche, Y., Ramstein, G., Braconnot, P., Marti, O., and Cortijo, E.: Simulating the amplification of orbital forcing by ocean feedbacks in the last glaciation, Nature, 410, 570–574, 2001.

Khodri, M., Ramstein, G., de Noblet-Ducoudre, N., and Kageyama, M.: Sensitivityof the Northern extratropics hydrological cycle to the changing insolation forcing at the 126 and 115 ky BP, Clim. Dynam., 21, 273–287, 2003.

Kiefer, T., Sarnthein, M., Erlenkeuser, H., Grootes, P. M., and Roberts, A. P.: North Pacific response to millennial-scale in the ocean circulation in the last 60 ka, Paleoceanography 16(2), 179–189, 2001.

Knutti, R., Flückiger, J., Stocker, T. F., and Timmermann, A.: Strong hemispheric coupling of glacial climate through freshwater discharge and ocean circulation, Nature, 430, 851–856, 2004.

Kobashi, T., Severinghaus, J. P., Brook, E. J., Barnola, J. M., and Grachev, A. M.: Precise timing and characterization of abrupt climate change 8200 years ago from air trapped in polar ice, Quaternary Sci. Rev., 26, 1212–1222, 2007.

Krinner, G., Genthon, C., and Jouzel, J.: GCM analysis of local influences on ice core δ signals, Geophys. Res. Lett., 24, 2825–2828, 1997.

Landais, A.: Variabilité climatique rapide en Atlantique Nord: l'apport des isotopes de l'air piégé dans la glace du Groenland, Thèse de doctorat de l'Université Paris, 6, 305 pp., 2004.

Landais, A., Barnola, J. M., Masson-Delmotte, V., Jouzel, J., Chappellaz, J., Caillon, N., Huber, C., Leuenberger, M., and Johnsen, S. J.: A continuous record of temperature evolution over a sequence of Dansgaard-Oeschger events during Marine Isotopic Stage 4 (76 to 62 kyr BP), Geophys. Res. Lett., 31, L22211.1-L22211.4, doi:10.1029/2004GL021193, 2004a.

Landais, A., Caillon, N., Goujon, C., Grachev, A. M., Barnola, J.

M., Chappellaz, J., Jouzel, J., Masson-Delmotte, V., and Leuenberger, M.: Quantification of rapid temperature change during DO event 12 and phasing with methane inferred from air isotopic measurements, Earth Planet. Sc. Lett., 225, 221–232, 2004b.

Landais, A., Caillon, N., Severinghaus, J., Barnola, J.-M., Goujon, C., Jouzel, J., and Masson-Delmotte, V.: Isotopic measurements of air trapped in ice to quantify temperature changes, C. R. Geosci., 336, 963–970, 2004c.

Landais, A., Masson-Delmotte, V., Jouzel, J., Raynaud, D., Johnsen, S., Huber, C., Leuenberger, M., Schwander, J., and Minster, B.: The glacial inception as recorded in the NorthGRIP Greenland ice core: timing, structure and associated abrupt temperature changes, Clim. Dynam. 26, 273–284, 2006.

Landais, A., Dreyfus, D., Capron, E., Sanchez-Goni, M. F., Desprat, S., Jouzel, J., Hoffmann, G., and Johnsen, S.: What drive orbital- and millennial-scale variations of the δ^{18}O of atmospheric oxygen ?, Quaternary Sci. Rev., 29, 235–246, 2010.

Lang, C., Leuenberger, M., Schwander, J., and Johnsen, S.: 16 °C rapid temperature variation in central Greenland 70 000 years ago, Science, 286, 934–937, 1999.

Laskar, J., Robutel, P., Joutel, F., Gastineau, M., Correia, A. C. M., and Levrard, B.: A long-term numerical solution for the insolation quantities of the Earth, A&A 428, 261–285, 2004.

Leuenberger, M. C., Lang, C., and Schwander, J.: δ^{15}N measurements as a calibration tool for the paleothermometer and gas–ice age differences: a case study for the 8200 BP event on GRIP ice, J. Geophys. Res.-Atmospheres, 104, 22163–22170, 1999.

Levermann, A., Schewe, J., and Montoya, M.: Lack of bipolar seesaw in response to Southern Ocean wind reduction, Geophys. Res. Lett., 34, L12711, doi:10.1029/2007GL030255., 2007.

Li, C., Battisti, D. S., Schrag, D. P., and Tziperman, E.: Abrupt climate shifts in Greenland due to displacements of the sea ice edge, Geophys. Res. Lett., 32, L19702, doi:10.1029/2005GL023492, 2005.

Lisiecki, L. E. and Raymo, M. E.: A Pliocene-Pleistocene stack of 57 globally distributed benthic delta O-18 records, Paleoceanography, 20, PA1003, doi:10.1029/2004PA001071., 2005.

Liu, Z., Otto-Bliesner, B. L., He, F., Brady, E. C., Tomas R., Clark, P. U., Carlson, A. E., Lynch-Stieglitz, J., Curry, W., Brook, E., Erickson, D., Jacob, R., Kutzbach, J., and Cheng, J.: Transient Simulation of Last Deglaciation with a New Mechanism for Bølling-Allerød Warming, Science, 325, 310–314, 2009.

Lorius, C. and Merlivat, L.: Distribution of mean surface stable isotope values in East Antarctica. Observed changes with depth in a coastal area, in: Isotopes and impurities in snow and ice, edited by: IAHS Publication, Vienna, IAHS, 125–137, 1977.

Loulergue, L., Schilt, A., Spahni, R., Masson-Delmotte, V., Blunier, T., Lemieux, B., Barnola, J.-M., Raynaud, D., Stocker, T. F., and Chappellaz, J.: Orbital and millennial-scale features of atmospheric CH_4 over the past 800 000 years, Nature, 453, 383–386, 2008.

Lüthi, D., Le Floch, M., Bereiter, B., Blunier, T., Barnola, J.-M., Siegenthaler, U., Raynaud, D., Jouzel, J., Fischer, H., Kawamura, K., and Stocker, T. F.: High-resolution carbon dioxide concentration record 650 000–800 000 years before present, Nature, 453, 379–382, 2008.

MacAyeal, D. R.: Binge/purge oscillations of the Laurentide ice sheet as a cause of the North Atlantic's Heinrich events, Paleoceanography, 8, 775–784, 1993.

Margari, V., Skinner, L. C., Tzedakis, P. C., Ganopolski, A., Vautravers, M., and Shackleton, N. J.: The nature of millennial-scale climate variabilityduring the past two glacial periods, Nat. Geosci., 3, 127–131, 2010.

Mariotti, A.: Atmospheric nitrogen as a reliable stable standard for ^{15}N abundance measurements, Nature, 303, 685–687, 1983.

Masson-Delmotte, V., Stenni, B., and Jouzel, J.: Common millenial scale variability of Antarctic and southern ocean temperatures during the past 5000 years reconstructed from EPICA Dome C ice core, The Holocene, 14, 145–151, 2004.

Masson-Delmotte, V., Jouzel, J., Landais, A., Stievenard, M., Johnsen, S. J., White, J. W. C., Sveinbjornsdottir, A., and Fuhrer, K.: Deuterium excess reveals millennial and orbital scale fluctuations of Greenland moisture origin, Science, 309, 118–121, 2005a.

Masson-Delmotte, V., Landais, A., Stievenard, M., Cattani, O., Falourd, S., Jouzel J., Johnsen, S., Dahl-Jensen, D., Sveinbjornsdottir, A., White, J. W. C., Popp, T., and Fischer, H.: Holocene climatic changes in Greenland: different deuterium excess signals at Greenland Ice Core Project (GRIP) and NorthGRIP, J. Geophys. Res., 110, doi:10.1029/2004JD005575, 2005b.

Masson-Delmotte, V., Hou, S., Ekaykin, A., Jouzel, J., Aristarain, A., Bernardo, R. T., Bromwich, D., Cattani, O., Delmotte, M., Falourd, S., Frezzotti, M., Gallée, H., Genoni, L., Isaksson, E., Landais, A., Helsen, M. M., Hoffmann, G., Lopez, J., Morgan, V., Motoyama, H., Noone, D., Oerter, H., Petit, J. R., Royer, A., Uemura, R., Schmidt, G. A., Schlosser, E., Simões, J. C., Steig, E. J., Stenni, B., Stievenard, M., van den Broeke, M. R., van de Wal, R. S. W., van de Berg, W. J., Vimeux, F., and White, J. W. C.: A review of Antarctic surface snow isotopic composition: observations, atmospheric circulation and isotopic modelling, J. Climate, 21, 3359–3387, 2008.

McManus, J. F., Bond, G. C., Broecker, W. S., Johnsen, S. J., Labeyrie, L., and Higgins, S.: High-resolution climatic records from the North Atlantic during the last interglacial, Nature, 371, 326–329, 1994.

McManus, J. F., Oppo, D. W., and Cullen, J.-L.: A 0.5-Million-Year Record of the millennial-scale climate variability in the North Atlantic, Science, 283, 971–975, 1999.

Meyer, H., Schönicke, L., Wand, U., Hubberten, H.-W., and Friedrichsen, H.: Isotope studies of hydrogen and oxygen in ground ice ? Experiences with the equilibration technique, Isot. Environ. Health S., 36, 133–149, 2000.

Meyer, M. C., Spötl, C., and Magini, A.: The demise of the last interglacial recorded in isotopically speleothems from the Alps, Quaternary Sci. Rev., 27, 476–496, 2008.

Monnin, E., Indermühle, A., Dällenbach, A., Flückiger, J., Stauffer, B., Stocker, T. F., Raynaud, D., and Barnola, J.-M.: Atmospheric CO_2 concentrations over the last glacial terminaison, Science, 291, 112–114, 2001.

NorthGRIP-community-members: High-resolution record of Northern Hemisphere climate extending into the last interglacial period, Nature, 431, 147-151, 2004.

Oerter, H., Graf, W., Meyer, H., and Wilhelms, F.: The EPICA ice core from Dronning Maud Land: first results from stable-isotope measurements, Ann. Glaciol., 39, 307–312, 2004.

Oppo, D. W., Lloyd, D., Keigwin, L. D., and McManus, J. F.: Persistent suborbital climate variability in marine isotope stage 5 and Termination II, Paleoceanography, 16, 280–292, 2001.

Pahnke, K., Zahn, R., Elderfield, H., and Schulz, M.: 340 000-year centennial-scale marine record of Southern Hemisphere climatic oscillation, Science, 301, 948–952, 2003.

Parrenin, F., Barnola, J.-M., Beer, J., Blunier, T., Castellano, E., Chappellaz, J., Dreyfus, G., Fischer, H., Fujita, S., Jouzel, J., Kawamura, K., Lemieux-Dudon, B., Loulergue, L., Masson-Delmotte, V., Narcisi, B., Petit, J.-R., Raisbeck, G., Raynaud, D., Ruth, U., Schwander, J., Severi, M., Spahni, R., Steffensen, J. P., Svensson, A., Udisti, R., Waelbroeck, C., and Wolff, E.: The EDC3 chronology for the EPICA Dome C ice core, Clim. Past, 3, 485–497, doi:10.5194/cp-3-485-2007, 2007.

Parrenin, F., Dreyfus, G., Durand, G., Fujita, S., Gagliardini, O., Gillet, F., Jouzel, J., Kawamura, K., Lhomme, N., Masson-Delmotte, V., Ritz, C., Schwander, J., Shoji, H., Uemura, R., Watanabe, O., and Yoshida, N.: 1-D-ice flow modelling at EPICA Dome C and Dome Fuji, East Antarctica, Clim. Past, 3, 243–259, doi:10.5194/cp-3-243-2007, 2007.

Peterson, L. C., Haug, G. H., Hughen, K. A., and Röhl, U.: Rapid Changes in the Hydrologic Cycle of the Tropical Atlantic During the Last Glacial, Science, 290, 1947–1951, 2000.

Petit, J. R., Jouzel, J., Raynaud, D., Barkov, N. I., Barnola, J.-M., Basile, I., Bender, M., Chappellaz, J., Davis, M., Delaygue, G., Delmotte, M., Kotlyakov, V. M., Legrand, M., Lipenkov, V. Y., Lorius, C., Pepin, L., Ritz, C., Saltzman, E., and Stievenard, M.: Climate and atmospheric history of the past 420,000 years from the Vostok ice core, Antarctica, Nature, 399, 429–436, 1999.

Rahmstorf, S.: Timing of abrupt climate change: A precise clock, Geophys. Res. Lett., 30(10), 1050, doi:10.1029/2003GL017115, 2003.

Rind, D., Demenocal, P., Russell, G. L., Sheth, S., Collins, D., Schmidt, G. A., and Teller, J.: Effects of glacial meltwater in the GISS Coupled Atmosphere-Ocean Model: Part I: North Atlantic Deep Water response, J. Geophys. Res., 106, 27335–27354, 2001.

Rousseau, D. D., Kukla, G., and McManus, J.: What is what in the ice and the ocean?, Quaternary Sci. Rev., 25, 2025–2030, 2006.

Ruth, U., Barnola, J.-M., Beer, J., Bigler, M., Blunier, T., Castellano, E., Fischer, H., Fundel, F., Huybrechts, P., Kaufmann, P., Kipfstuhl, S., Lambrecht, A., Morganti, A., Oerter, H., Parrenin, F., Rybak, O., Severi, M., Udisti, R., Wilhelms, F., and Wolff, E.: "EDML1": a chronology for the EPICA deep ice core from Dronning Maud Land, Antarctica, over the last 150 000 years, Clim. Past, 3, 475–484, doi:10.5194/cp-3-475-2007, 2007.

Sanchez-Goñi, M. F., Turon, J.-L., Eynault, F., and Gendreau, S.: European climatic response to millennial-scale changes in the atmosphere-ocean system during the last glacial period, Quaternary Res., 54, 394–403, 2000.

Sanchez-Goñi, M. F., Cacho, I., Turon, J.-L., Guiot, J., Sierro, F. J., Peyrouquet, J.-P., and Shackleton, N. J.: Synchroneity between marine and terrestrial responses to millennial scale climatic variability during the last glacial period in the Mediterranean region, Clim. Dynam., 19, 95–105, 2002.

Schulz, M.: On the 1470-year pacing of Dansgaard-Oeschger warm events, Paleoceanography, 17, 4.1–4.10, 2002.

Schulz, M., Paul, A., and Timmermann, A.: Relaxation oscillators in concert: A framework for climate change at millennial timescales during the late Pleistocene, Geophys. Res. Lett., 29(24), 2193, doi:10.1029/2002GL016144, 2002.

Severi, M., Becagli, S., Castellano, E., Morganti, A., Traversi, R., Udisti, R., Ruth, U., Fischer, H., Huybrechts, P., Wolff, E., Parrenin, F., Kaufmann, P., Lambert, F., and Steffensen, J. P.: Synchronisation of the EDML and EDC ice cores for the last 52 kyr by volcanic signature matching, Clim. Past, 3, 367–374, doi:10.5194/cp-3-367-2007, 2007.

Severinghaus, J. P., Sowers, T., Brook, E. J., Alley, R. B., and Bender, M. L.: Timing of abrupt climate change at the end of the Younger Dryas interval from thermally fractionated gases in polar ice, Nature, 391, 141–146, 1998.

Severinghaus, J. P. and Brook, E. J.: Abrupt climate change at the end of the last glacial period inferred from trapped air in polar ice, Science, 286, 930–934, 1999.

Shackleton, N. J. and Pisias, N. G.: Atmospheric carbon dioxide, orbital forcing, and climate, Geoph. Monog. Series, 32, 412–417, 1985.

Shackleton, N. J.: Oxygen isotopes, ice volume and sea level, Quaternary Sci. Rev., 6, 183–190, 1987.

Shackleton, N. J., Sanchez-Goni, M. F., Pailler, D., and Lancelot, Y.: Marine isotope substage 5e and the Eemian interglacial, Global Planetary Changes, 36, 151–155, 2003a.

Shackleton, N. J., Sanchez Goñi, M. F., Pailler D., and Lancelot, Y.: Marine isotopic Substage 5e and the Eemian interglacial, Global Planetary Changes, 36, 151–155, 2003b.

Siddall, M., Thomas, F., Stocker, T., Blunier, T., Spahni, R., Schwander, J., Barnola, J.-M., and Chappellaz, J.: Marine Isotope Stage (MIS) 8 millennial variability stratigraphically identical to MIS 3, Paleoceanography 22, PA1208, doi:10.1029/2006PA001345, 2007.

Sime, L. C., Wolff, E. W., Oliver, K. I. C., and Tindall, J. C.: Evidence for warmer interglacials, Nature, 462, 342–345, 2009.

Sprovieri, R., Di Stefano, E., Alessandro Incarbona, A., and Oppo, D. W.: Suborbital climate variability during Marine Isotopic Stage 5 in the central Mediterranean basin: evidence from calcareous plankton record, Quaternary Sci. Rev., 25, 2332–2342, 2006.

Steffensen, J. P., Andersen, K. K., Bigler, M., Clausen, H. B., Dahl-Jensen, D., Fischer, H., Goto-Azuma, K., Hansson, M., Johnsen, S. J., Jouzel, J., Masson-Delmotte, V., Popp, T., Rasmussen, S. O., Röthlisberger, R., Ruth, U., Stauffer, B., Siggaard-Andersen, M.-L., Sveinbjörnsdóttir, A. E., Svensson, A., and White, J. W. C.: High-Resolution Greenland Ice Core Data Show Abrupt Climate Change Happens in Few Years, Science, 321, 680–683, 2008.

Stenni, B., Masson-Delmotte, V., Johnsen, S., Jouzel, J., Longinelli, A., Monnin, E., Röthlisberger, R., and Selmo, E.: An oceanic cold reversal during the last deglaciation, Science, 293, 2074–2077, 2001.

Stenni, B., Selmo, E., Masson-Delmotte, V., Oerter, H., Meyer, H., Röthlisberger, R., Jouzel, J., Cattani, O., Falourd, S., Fischer, H., Hoffmann, G., Lacumin, P., Johnsen, S. J., and Minster, B.: The deuterium excess records of EPICA Dome C and Dronning Maud Land ice cores (East Antarctica), Quaternary Sci. Rev., 29, 146–159, 2010.

Stocker, T. F., Wright, D. G., and Mysak, L. A.: A zonally averaged, coupled ocean-atmosphere model for paleoclimate studies, J. Climate, 5, 773–797, 1992.

Stocker, T. F., and Johnsen, S. J.: A minimum thermodynamic model for the bipolar seesaw, Paleoceanography, 18, 1087, 8 pp., 2003.

Svensson, A., Andersen, K. K., Bigler, M., Clausen, H. B., Dahl-Jensen, D., Davies, S. M., Johnsen, S. J., Muscheler, R., Parrenin, F., Rasmussen, S. O., Röthlisberger, R., Seierstad, I., Steffensen, J. P., and Vinther, B. M.: A 60 000 year Greenland stratigraphic ice core chronology, Clim. Past, 4, 47–57, doi:10.5194/cp-4-47-2008, 2008.

Swingedouw, D., Fichefet, T., Goosse, H., and Loutre, M. F.: Impact of transient freshwater releases in the Southern Ocean on the AMOC and climate, Clim. Dynam., 33, 365–381, 2009.

Taylor, K. C., White, J. W. C., Severinghaus, J. P., Brook, E. J., Mayewski, P. A., Alley, R. B., Steig, E. J., Spencer, M. K., Meyerson, E., Meese, D. A., Lamorey, G. W., Grachev, A., Gow, A. J., and Barnett, B. A.: Abrupt climate change around 22 ka on the Siple Coast of Antarctica, Quaternary Sci. Rev., 23, 7–15, 2004.

Thomas, E. R., Wolff, E. W., Mulvaney, R., Steffensen, J. P., Johnsen, S. J., Arrowsmith, C., White, J. W. C., Vaughn, B., and Popp, T.: The 8.2 ka event from Greenland ice cores, Quaternary Sci. Rev., 26, 70–81, 2007.

van Kreveld, S. A., Sarnthein, M., Erlenkeuser, H., Grootes, P., Jung, S., Nadeau, M. J., Pflaumann, U., and Voelker, A. H. L.: Potential links between surging ice sheets, circulation changes and the Dansgaard-Oeschger cycles in the Irminger Sea, 60–18 kyr, Paleoceanography, 15, 425–442, 2000.

Velinga, M. and Wood, R. A.: Global climatic impacts of a collapse of the Atlantic thermohaline circulation, Climatic Change, 54, 251–267, 2002.

Vimeux, F., Cuffey, K., and Jouzel, J.: New insights into Southern Hemisphere temperature changes from Vostok ice cores using deuterium excess correction over the last 420 000 years, Earth Planet. Sc. Lett., 203, 829–843, 2002.

Vinther, B. M., Buchardt, S. L., Clausen, H. B., Dahl-Jensen, D., Johnsen, S. J., Fisher, D. A., Koerner, R. M., Raynaud, D., Lipenkov, V., Andersen, K. K., Blunier, T., Rasmussen, S. O., Steffensen, J. P., and Svensson, A. M.: Holocene thinning of the Greenland ice sheet, Nature, 461, 385–388, 2009.

Voelker, A. H. L.: Global distribution of centennial-scale records for Marine Isotope Stage (MIS) 3: a database, Quaternary Sci. Rev., 21, 1185–1212, 2002.

von Grafenstein, U., Erlenkeuser, H., Müller, J., Jouzel J., and Johnsen, S. J.: The cold event 8200 years ago documented in oxygen isotope records of precipitation in Europe and Greenland, Clim. Dynam., 14, 73–81, 1998.

Waelbroeck, C., Labeyrie, L., Michel, E., Duplessy, J. C., McManus, J. F., Lambeck, K., Balbon, E., and Labracherie, M.: Sea-level and deep water temperature changes derived from benthic foraminifera isotopic records, Quaternary Sci. Rev., 21, 295–305, 2002.

Wang, Y., Cheng, H., Edwards, R. L., Kong, X., Shao, X., Chen, S., Wu, J., Jiang, X., Wang, X., and An, Z.: Millennial- and orbital-scale changes in the East Asian monsoon over the past 224 000 years, Nature, 451, 1090–1093, 2008.

Wang, Y. J., Cheng, H., Edwards, R. L., An, Z. S., Wu, J. Y., Shen, C.-C., and Dorale, J. A.: A High-Resolution Absolute-Dated Late Pleistocene Monsoon Record from Hulu Cave, China, Science, 94, 234–2348, 2001.

Wang, Z. and Mysak, L. A.: Glacial abrupt climate changes and Dansgaard-Oeschger oscillations in a coupled climate model, Paleoceanography, 21, PA2001, doi:10.1029/2005PA001238, 2006.

Weirauch, D., Billups, K., and Martin, P.: Evolution of millennial-scale climate variability during the mid-Pleistocene, Paleoceanography, 23, PA3216, doi:10.1029/2007PA001584, 2008.

Wolff, E. W., Chappellaz, J., Blunier, T., Rasmussen, S. O., and Svensson, A.: Millennial-scale variability during the last glacial: The ice core record, Quaternary Sci. Rev., doi:10.1016/j.quascirev.2009.10.013, in press, 2009a.

Wolff, E. W., Fischer, H., and Röthlisberger, R.: Glacial terminations as southern warmings without northern control, Nat. Geosci., 2, 206–209, 2009b.

Wunsch, C.: Abrupt climate change: An alternative view, Quaternary Res., 65, 191–203, 2006.